Published for SISSA by Springer

Received: November 22, 2022
Revised: March 9, 2023
Accepted: April 17, 2023
Published: April 28, 2023

On SYK traversable wormhole with imperfectly correlated disorders

Tomoki Nosaka[a] **and Tokiro Numasawa**[b]

[a] *Kavli Institute for Theoretical Sciences, University of Chinese Academy of Sciences, Beijing, 100190, China*
[b] *Institute for Solid State Physics, University of Tokyo, Kashiwa 277-8581, Japan*

E-mail: nosaka@yukawa.kyoto-u.ac.jp, numasawa@issp.u-tokyo.ac.jp

Abstract: In this paper, we study the phase structure of two Sachdev-Ye-Kitaev models (L-system and R-system) coupled by a simple interaction, with imperfectly correlated disorder. When the disorder of the two systems is perfectly correlated, $J^{(L)}_{i_1\cdots i_q} = J^{(R)}_{i_1\cdots i_q}$, this model is known to exhibit a phase transition at a finite temperature between the two-black hole phase at high temperature and the traversable wormhole phase at low temperature. We find that, as the correlation $\langle J^{(L)}_{i_1\cdots i_q} J^{(R)}_{i_1\cdots i_q}\rangle$ is decreased, the critical temperature becomes lower. At the same time, the transmission between the L-system and R-system in the low-temperature phase becomes more suppressed, while the chaos exponent of the whole system becomes larger. Interestingly we also observe that when the correlation is smaller than some q-dependent critical value the phase transition completely disappears in the entire parameter space. At zero temperature, the energy gap becomes larger as we decrease the correlation. We also use a generalized thermofield double state as a variational state. Interestingly, this state coincides with the ground state in the large q limit.

Keywords: AdS-CFT Correspondence, Black Holes in String Theory, Holography and Condensed Matter Physics (AdS/CMT), Random Systems

ArXiv ePrint: 2210.13123

https://doi.org/10.1007/JHEP04(2023)145

JHEP04(2023)145

Contents

JHEP04(2023)145

1 Introduction and summary

The Sachdev-Ye-Kitaev (SYK) model [1, 2] is a useful model to study various aspects of strongly coupled many body systems. Moreover, the SYK model is also a toy model of a quantum black hole [3]. Both theories show the same pattern of conformal symmetry breaking at low energy and are described by the so-called Schwarzian action. This gives a concrete connection between the two theories.

Related to black holes, the SYK model also plays an important role to understand wormhole configurations in gravity. Two kinds of wormholes play important roles in the literature. The first one is the spatial wormhole. Spatial wormholes are related to entanglement [4–6]. In the context of AdS/CFT correspondence, the area of the wormhole connecting distant regions corresponds to entanglement entropy in CFT [7–9]. Moreover, it is expected that spatial wormholes are dual to entanglement between CFTs [5, 6] and the spacetime is built from entanglement [10, 11]. The other kind of wormhole is the spacetime wormhole or Euclidean wormhole. These are kinds of gravitational instanton and these spacetime wormholes are related to random couplings [12–14]. The SYK model is a model with random couplings and the wormhole configurations associated with a pattern of random couplings are studied [15, 16]. These Euclidean wormholes also appear in the context of the calculation of (Rényi) entanglement entropy. These are known as replica wormholes [17, 18] and play important roles in the context of black hole information problems.[1] Actually, two types of wormholes have also connections. For example, considering static spatial wormholes in Euclidean time, we get Euclidean wormholes. Those setups are interesting because by taking a different analytic continuation of those Euclidean wormholes we obtain a cosmological spacetime [20–24], which is originally pointed out in [25].

Usually, we assume that the random couplings of copies of SYK models have the same couplings, i.e., in each realization of the random couplings we use the same realization for all of the copies. This is a natural setup when we use the replica method to study the Rényi entropy for example. However, to study entangled states we can also consider the situation where the copies of SYK models have different random couplings. For example, if we simulate the SYK models on quantum computers it may be natural to consider different realizations because of errors etc.

Motivated by the above questions, we study the coupled SYK models where the two SYK models have different realizations of random couplings. The two-coupled SYK model was first considered in [31], with the two random couplings perfectly correlated, as the holographic dual of the global AdS_2 spacetime (eternal traversable wormhole), which is the static version of the wormhole formation process by the bulk non-local interaction [3, 32]. In the setup of [31], for the wormhole to become traversable, or on the SYK side the quantum teleportation to be successful, it is crucial for the state of the whole system to be the thermofield double state [33]. It was found that the ground state of the coupled SYK model is close to the thermofield double state [31, 34, 35], which ensures that the low-temperature dynamics of the model can be related to the traversable wormhole. Indeed,

[1] Recent developments in various aspects of wormhole geometries are also summarized in a review article [19].

JHEP04(2023)145

the coupled SYK model in the canonical ensemble exhibits a Hawking-Page-like phase transition between the high-temperature phase dual to the two-sided AdS_2 black hole and the low-temperature phase dual to the global AdS_2.

When the couplings of the two systems are different, it is not clear how to interpret the entanglement structure of the ground state and whether the system is dual to the traversable wormhole at low temperatures or not. It was also found in [36, 37] that the coupled SYK model does not exhibit a phase transition when the two random couplings are completely independent. Hence the correlation of the couplings is indeed important for the wormhole formation, and it is a non-trivial question how much correlation would be necessary for the wormhole to be formed.

More concretely, we consider the model where the two random couplings $J^{(L)}_{i_1\cdots i_q}$ and $J^{(R)}_{i_1\cdots i_q}$ obey the same Gaussian distribution while the two realizations are not completely identical, which we quantify by $\langle J^{(L)}_{i_1\cdots i_q} J^{(R)}_{i_1\cdots i_q}\rangle$ normalized by $\langle (J^{(L)}_{i_1\cdots i_q})^2\rangle$ $(= \langle (J^{(R)}_{i_1\cdots i_q})^2\rangle)$. By analyzing this model in the large N limit, we find the following results:

(i) As the correlation between the two random couplings is decreased, the critical temperature for the Hawking-Page-like phase transition becomes lower. This result can also be rephrased that the strength of the LR coupling required for reaching the wormhole phase at fixed temperature becomes higher, hence both the correlation of random couplings and direct LR coupling make it easy to create a wormhole configuration. This is also consistent with the fact that the wormhole phase exists even without direct LR coupling if the two random couplings are *super-correlated*, $\langle J^{(L)}_{i_1\cdots i_q} J^{(R)}_{i_1\cdots i_q}\rangle > \langle (J^{(L)}_{i_1\cdots i_q})^2\rangle$ [38–42].

(ii) We also observe that the phase transition completely disappears when the correlation between $J^{(L)}_{i_1\cdots i_q}$ and $J^{(R)}_{i_1\cdots i_q}$ is smaller than a non-zero finite value. Technically this occurs in the following way. Already in the original setup where the two random couplings are identical, there is no phase transition when the LR coupling is larger than some critical value: when the LR coupling is too large, even at a high temperature the dynamics are approximately the same as that for the model without SYK interaction which does not exhibit phase transition. We find that this critical value of the LR coupling becomes smaller as the correlation between $J^{(L)}_{i_1\cdots i_q}$ and $J^{(R)}_{i_1\cdots i_q}$ is decreased, and reaches zero before the two random couplings become completely independent. At the large q limit, we also estimate when the phase transition disappears as we decrease the correlation of random couplings between two sides.

(iii) We also evaluate the transmission amplitude T_{LR} between the L-side and the R-side in the low-temperature wormhole phase, and found that for the same temperature and the strength of the LR coupling, T_{LR} becomes smaller as the correlation between $J^{(L)}_{i_1\cdots i_q}$ and $J^{(R)}_{i_1\cdots i_q}$ is decreased. On the other hand, the chaos exponent λ_L, which is non-zero even in the wormhole phase, becomes larger as the correlation of the random couplings is decreased. These two results are reasonable if λ_L of this model measures the speed at that a simple initial excitation spread within a single side, which would be suppressed if the excitation leaks to the other side.

JHEP04(2023)145

We observe the results (i-iii) numerically for $q = 4$ and also confirm the results (i, ii) analytically in the large q limit.

The organization of this paper is as follows. In section 2, we clarify the model we study in this paper and write the partition function in the large N limit with the bilocal field formalism. By using the bilocal field formalism, we analyze how the large N phase structure and various properties of each phase are modified by the imperfect correlation of disorders for finite q in section 3 and in the large q limit in section 4. In section 5 we study the structure of the ground state of the coupled system for $\langle J^{(L)}_{i_1\cdots i_q} J^{(R)}_{i_1\cdots i_q}\rangle < \langle (J^{(L)}_{i_1\cdots i_q})^2\rangle$ which generalizes the structure of the thermofield double state for $J^{(L)}_{i_1\cdots i_q} = J^{(R)}_{i_1\cdots i_q}$. In section 6 we summarize our results and list possible future directions of research. Some technical details of the calculation in the large q limit are collected in appendix A.

2 $J^{(L)}_{i_1\cdots i_q} \neq J^{(R)}_{i_1\cdots i_q}$ model

In this paper we consider a $(0+1)$-dimensional quantum mechanics with the following disordered Hamiltonian:[2]

$$H = H^{(L)}_{\rm SYK} + H^{(R)}_{\rm SYK} + \mu H_{\rm int}, \tag{2.1}$$

where

$$H^{(L)}_{\rm SYK} = i^{\frac{q}{2}} \sum_{i_1<i_2<\cdots<i_q}^{N} J^{(L)}_{i_1 i_2\cdots i_q} \psi^L_{i_1}\psi^L_{i_2}\cdots\psi^L_{i_q}, \quad H^{(R)}_{\rm SYK} = i^{\frac{q}{2}}(-1)^{\frac{q}{2}} \sum_{i_1<i_2<\cdots<i_q}^{N} J^{(R)}_{i_1 i_2\cdots i_q} \psi^R_{i_1}\psi^R_{i_2}\cdots\psi^R_{i_q},$$
$$H_{\rm int} = i\sum_{i=1}^{N} \psi^L_i \psi^R_i, \tag{2.2}$$

$\{\psi^a_i, \psi^b_j\} = \delta_{ab}\delta_{ij}$ $(a = L, R)$, and $J^{(a)}_{i_1 i_2\cdots i_q}$ are random couplings drawn from the Gaussian distribution with the following mean and variance:

$$\langle J^{(a)}_{i_1 i_2\cdots i_q}\rangle = 0, \quad \langle J^{(a)}_{i_1 i_2\cdots i_q} J^{(a)}_{j_1 j_2\cdots j_q}\rangle = \frac{\mathcal{J}^2\cdot 2^{q-1}(q-1)!}{q\cdot N^{q-1}} \delta_{i_1 j_1}\delta_{i_2 j_2}\cdots\delta_{i_q j_q}. \tag{2.3}$$

Here $J^{(a)}_{i_1 i_2\cdots i_q}$ are drawn independently for different sets of subscripts $i_1 i_2\cdots i_q$. On the other hand, with respect to $a = L, R$, we consider the case where $J^{(L)}_{i_1 i_2\cdots i_q}$ and $J^{(R)}_{i_1 i_2\cdots i_q}$ are imperfectly correlated with each other:

$$\langle J^{(L)}_{i_1 i_2\cdots i_q} J^{(R)}_{j_1 j_2\cdots j_q}\rangle = \frac{\tilde{\mathcal{J}}^2\cdot 2^{q-1}(q-1)!}{q\cdot N^{q-1}} \delta_{i_1 j_1}\delta_{i_2 j_2}\cdots\delta_{i_q j_q}, \tag{2.4}$$

with $0 \le \tilde{\mathcal{J}} \le \mathcal{J}$.[3] See figure 1 for an example of the Feynman diagrams affected by this deformation. This partial correlation can be realized by drawing two independent

[2] Although we do not investigate in this paper, it would be also interesting to study how the correlation between the disorders affects the two-coupled SYK model with Dirac fermions (so-called complex SYK model) [43] whose phase structure was analyzed in [44, 45] when the random couplings on two sites are set to be identical.

[3] One may also consider the case $\tilde{\mathcal{J}} > \mathcal{J}$, where the Hamiltonian is non-Hermitian [38–42].

JHEP04(2023)145

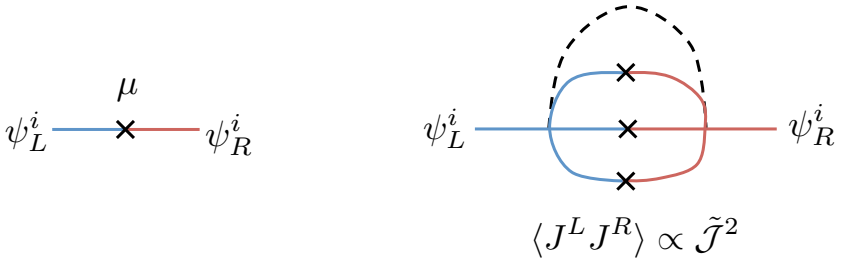

Figure 1. *Left*: a diagram that is not affected by the random couplings. *Right*: a typical diagram whose contribution is reduced when we decrease the correlation between the left random couplings and the right random couplings.

random variables $J^{(\alpha)}_{i_1 i_2 \cdots i_q}$ $(\alpha = 1, 2)$ from the same distribution as $J^{(L)}_{i_1 i_2 \cdots i_q}$ (2.3) and writing $J^{(a)}_{i_1 i_2 \cdots i_q}$ as

$$\begin{aligned} J^{(L)}_{i_1 i_2 \cdots i_q} &= J^{(1)}_{i_1 i_2 \cdots i_q} \sqrt{\frac{1 + \tilde{\mathcal{J}}^2/\mathcal{J}^2}{2}} + J^{(2)}_{i_1 i_2 \cdots i_q} \sqrt{\frac{1 - \tilde{\mathcal{J}}^2/\mathcal{J}^2}{2}}, \\ J^{(R)}_{i_1 i_2 \cdots i_q} &= J^{(1)}_{i_1 i_2 \cdots i_q} \sqrt{\frac{1 + \tilde{\mathcal{J}}^2/\mathcal{J}^2}{2}} - J^{(2)}_{i_1 i_2 \cdots i_q} \sqrt{\frac{1 - \tilde{\mathcal{J}}^2/\mathcal{J}^2}{2}}. \end{aligned} \tag{2.5}$$

Consider the Euclidean partition function (annealed average) of this theory at finite temperature β^{-1}:

$$\begin{aligned} Z(\beta) &= \left\langle \int \mathcal{D}\psi^{(a)}_i(\tau) \exp\left[- \int d\tau \left(\sum_{a=L,R} \sum_{i=1}^{N} \frac{1}{2} \psi^a_i \partial_\tau \psi^a_i + H \right) \right] \right\rangle_{J^{(\alpha)}_{i_1 i_2 \cdots i_a}} \\ &= \mathcal{N}^{-1} \int \left(\prod_{\alpha=1,2} \prod_{i_1 < i_2 < \cdots < i_q}^{N} dJ^{(\alpha)}_{i_1 i_2 \cdots i_q} e^{-\frac{1}{2} \frac{q \cdot N^{q-1}}{\mathcal{J}^2 \cdot 2^{q-1} (q-1)!} (J^{(\alpha)}_{i_1 i_2 \cdots i_q})^2} \right) \\ &\quad \int \mathcal{D}\psi^{(a)}_i(\tau) \exp\left[- \int d\tau \left(\sum_{a=L,R} \sum_{i=1}^{N} \frac{1}{2} \psi^a_i \partial_\tau \psi^a_i + H \right) \right]. \end{aligned} \tag{2.6}$$

After the same manipulation as [37] we can rewrite the partition function in terms of the bilocal fields $G_{ab}(\tau, \tau')$ and $\Sigma_{ab}(\tau, \tau')$ as

$$Z(\beta) = \int \mathcal{D}G_{ab}(\tau, \tau') \mathcal{D}\Sigma_{ab}(\tau, \tau') e^{-S_E}, \tag{2.7}$$

where the effective action is

$$\begin{aligned} -S_E/N = \; & \log \mathrm{Pf} \left(- \delta(\tau - \tau') \partial_{\tau'} \delta_{ab} + \frac{\Sigma_{ab}(\tau, \tau') - \Sigma_{ba}(\tau', \tau)}{2} \right) \\ & - \frac{1}{2} \int d\tau d\tau' \sum_{a,b} \left[\Sigma_{ab}(\tau, \tau') G_{ab}(\tau, \tau') - s_{ab} \frac{\mathcal{J}^2_{ab}}{2q^2} [2 G_{ab}(\tau, \tau')]^q \right] \\ & + \frac{i\mu}{2} \int d\tau [-G_{LR}(\tau, \tau) + G_{RL}(\tau, \tau)]. \end{aligned} \tag{2.8}$$

JHEP04(2023)145

Here $s_{LL} = s_{RR} = 1$, $s_{LR} = s_{RL} = (-1)^{\frac{q}{2}}$ and $\mathcal{J}_{LL} = \mathcal{J}_{RR} = \mathcal{J}$, $\mathcal{J}_{LR} = \mathcal{J}_{RL} = \tilde{\mathcal{J}}$. The Schwinger-Dyson equations $\frac{\delta S_E}{\delta G_{ab}(\tau,\tau')} = \frac{\delta S_E}{\delta \Sigma_{ab}(\tau,\tau')} = 0$ are

$$\begin{aligned}
&\partial_\tau G_{ab}(\tau,\tau') - \sum_c \int d\tau'' \frac{\Sigma_{ac}(\tau,\tau'') - \Sigma_{ca}(\tau'',\tau)}{2} G_{cb}(\tau'',\tau') = \delta_{ab}\delta(\tau-\tau'), \\
&\Sigma_{ab}(\tau,\tau') = \frac{s_{ab}\mathcal{J}_{ab}^2}{q}(2G_{ab}(\tau,\tau'))^{q-1} + i\mu(-\delta_{aL}\delta_{bR} + \delta_{aR}\delta_{bL})\delta(\tau-\tau').
\end{aligned} \tag{2.9}$$

From the two equations it follows that

$$G_{ab}(\tau,\tau') = -G_{ba}(\tau',\tau). \tag{2.10}$$

By identifying $G_{ab}(\tau,\tau')$ with $(\alpha = 1,2)$

$$\begin{aligned}
G_{ab}(\tau,\tau') &= \frac{1}{N}\sum_{i=1}^N \langle \mathcal{T}\psi_i^a(\tau)\psi_i^b(\tau')\rangle_\beta \\
&= \begin{cases} \frac{1}{N\langle \mathrm{tr} e^{-\beta H}\rangle_{J^{(\alpha)}_{i_1\cdots i_q}}} \sum_{i=1}^N \langle \mathrm{tr} e^{\tau H}\psi_i^a e^{-H(\tau-\tau')}\psi_i^b e^{-(\tau'+\beta)H}\rangle_{J^{(\alpha)}_{i_1\cdots i_q}} & (\tau > \tau') \\ -\frac{1}{N\langle \mathrm{tr} e^{-\beta H}\rangle_{J^{(\alpha)}_{i_1\cdots i_q}}} \sum_{i=1}^N \langle \mathrm{tr} e^{\tau' H}\psi_i^b e^{-H(\tau'-\tau)}\psi_i^b e^{-(\tau+\beta)H}\rangle_{J^{(\alpha)}_{i_1\cdots i_q}} & (\tau < \tau') \end{cases},
\end{aligned} \tag{2.11}$$

we also find that $G_{ab}(\tau,\tau')$ obeys the following conditions[4]

$$G_{ab}(\tau,\tau')^* = -G_{ab}(-\tau,-\tau'), \quad G_{ab}(\tau+\beta,\tau') = -G_{ab}(\tau,\tau'). \tag{2.12}$$

From (2.11) and (2.9) it also follows that $G_{ab}(\tau,\tau'), \Sigma_{ab}(\tau,\tau')$ depends on τ,τ' only through $\tau-\tau'$, hence we may denote $G_{ab}(\tau,\tau')$ and $\Sigma_{ab}(\tau,\tau')$ respectively as $G_{ab}(\tau-\tau'), \Sigma_{ab}(\tau-\tau')$. Taking these into account, the Schwinger-Dyson equations (2.9) and the symmetry properties (2.10), (2.12) are written in a simpler way as

$$\begin{aligned}
&\partial_\tau G_{ab}(\tau) - \sum_c \int d\tau' \Sigma_{ac}(\tau-\tau')G_{cb}(\tau') = \delta_{ab}\delta(\tau), \\
&\Sigma_{ab}(\tau) = \frac{s_{ab}\mathcal{J}_{ab}^2}{q}(2G_{ab}(\tau))^{q-1} + i\mu(-\delta_{aL}\delta_{bR} + \delta_{aR}\delta_{bL})\delta(\tau),
\end{aligned} \tag{2.13}$$

$$G_{ab}(\tau) = -G_{ba}(-\tau), \quad G_{ab}(\tau)^* = -G_{ab}(-\tau), \quad G_{ab}(\tau+\beta) = -G_{ab}(\tau). \tag{2.14}$$

Note that when we set $\tilde{\mathcal{J}} = \mathcal{J}$, the effective action and the Schwinger-Dyson equation coincide with those in the Maldacena-Qi model [31] since the Hamiltonian reduces to the one in [31]. Also note that when we set $\tilde{\mathcal{J}} = 0$ the effective action and the Schwinger-Dyson equations coincide with those in the Kourkoulou-Maldacena model [46] if we identify $G_{LL}(\tau,\tau') = G_{RR}(\tau,\tau') = G_{\mathrm{diag}}(\tau,\tau')$, $G_{LR}(\tau,\tau') = G_{\mathrm{off}}(\tau,\tau')$.

By using the operator relations

$$\partial_\tau(e^{\tau H}\psi_i^a e^{-\tau H}\psi_i^a)|_{\tau\to+0} = [H,\psi_i^a]\psi_i^a = qH_{\mathrm{SYK}}^{(a)} + \mu H_{\mathrm{int}}, \quad (a = L,R) \tag{2.15}$$

[4]These arguments can be generalized to complex τ,τ' and we obtain $G_{ab}(u_1,u_2)^* = -G_{ab}(-u_1^*,-u_2^*)$, which we will use later in section 3.3.

JHEP04(2023)145

together with the identification (2.11), we can express the energy $E = \frac{\langle \mathrm{tr} H e^{-\beta H} \rangle_{J^{(\alpha)}_{i_1 \cdots i_q}}}{\langle \mathrm{tr} e^{-\beta H} \rangle_{J^{(\alpha)}_{i_1 \cdots i_q}}}$ as

$$\frac{E}{N} = \left[\frac{1}{q} \partial_\tau G_{LL}(\tau, 0) + \frac{1}{q} \partial_\tau G_{RR}(\tau, 0) + i\mu \left(1 - \frac{2}{q} \right) G_{LR}(\tau, 0) \right]_{\tau \to +0}. \tag{2.16}$$

Using the Schwinger-Dyson equations (2.13) and the symmetry property of $G_{ab}(\tau)$ (2.14) it follows

$$\lim_{\tau \to +0} \partial_\tau G_{aa}(\tau, 0) = \sum_c \int d\tau \Sigma_{ac}(\tau) G_{ca}(-\tau) = -\sum_c \frac{s_{ac} \mathcal{J}_{ac}^2}{2q} \int d\tau (2G_{ac}(\tau))^q, \tag{2.17}$$

hence the energy (2.16) can be further rewritten as

$$\frac{E}{N} = -\sum_{a,b} \frac{s_{ab} \mathcal{J}_{ab}^2}{2q^2} \int d\tau (2G_{ab}(\tau))^q + i\mu G_{LR}(0). \tag{2.18}$$

In the following sections, we study the solutions of the Schwinger-Dyson equations both numerically and analytically.

3 Finite q, large N

In this section, we study the two-coupled model (2.1) with $q = 4$ in the large N limit numerically by using the bilocal field formalism (2.7) with (2.8), (2.9).

3.1 Phase diagram

In the large N limit, we can evaluate the partition function (2.8) by the solution of the equations of motion (2.9). If we define the Fourier transformation as

$$f(\tau) \to \widehat{f}(\nu) = \int_0^\beta d\tau e^{i\nu\tau} f(\tau), \tag{3.1}$$

and also impose an ansatz $G_{RR}(\tau) = G_{LL}(\tau)$, the Euclidean Schwinger-Dyson equations (2.9) can be rewritten as

$$\begin{aligned}
&\widehat{G}_{LL}(\nu) + \frac{i\nu + \widehat{\Sigma}_{LL}(\nu)}{(i\nu + \widehat{\Sigma}_{LL}(\nu))^2 + \widehat{\Sigma}_{LR}(\nu)^2} = 0, \\
&\widehat{G}_{LR}(\nu) - \frac{\widehat{\Sigma}_{LR}(\nu)}{(i\nu + \widehat{\Sigma}_{LL}(\nu))^2 + \widehat{\Sigma}_{LR}(\nu)^2} = 0, \\
&\Sigma_{LL}(\tau) = \frac{\mathcal{J}^2}{q} (2G_{LL}(\tau))^{q-1}, \quad \Sigma_{LR}(\tau) = \frac{(-1)^{\frac{q}{2}} \tilde{\mathcal{J}}^2}{q} (2G_{LR}(\tau))^{q-1} + i\mu\delta(\tau).
\end{aligned} \tag{3.2}$$

The partition function, or the free energy $F = -\frac{1}{\beta} \log Z$, can be evaluated in the large N limit by the solutions of (3.2) as

$$F \approx \min \left\{ \frac{1}{\beta} S_E[G_{ab}(\tau, \tau'), \Sigma_{ab}(\tau, \tau')] \,\middle|\, (G_{ab}, \Sigma_{ab}) \text{: solution of (3.2)} \right\}. \tag{3.3}$$

JHEP04(2023)145

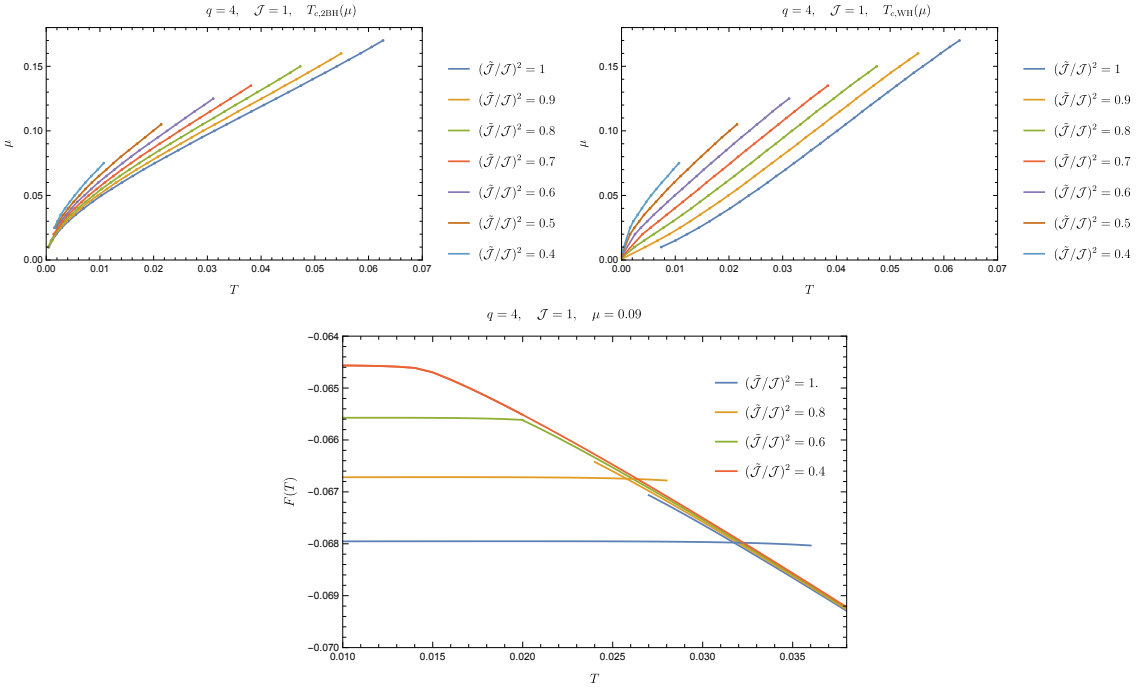

Figure 2. Top left/right: critical temperatures $T_{c,2\mathrm{BH}}(\mu)$ and $T_{c,\mathrm{WH}}(\mu)$ for various values of $\frac{\tilde{\mathcal{J}}}{\mathcal{J}}$. Bottom: free energy for the two solutions for $\mu = 0.09$ and various values of $\frac{\tilde{\mathcal{J}}}{\mathcal{J}}$ (for $\frac{\tilde{\mathcal{J}}^2}{\mathcal{J}^2} = 0.4$ the two solutions are smoothly connected with each other).

The set of equations (3.2) can be solved numerically for each value of $(q, \mathcal{J}, \tilde{\mathcal{J}}, \mu)$ and the inverse temperature $\beta = T^{-1}$. We performed the numerical analysis for $q = 4, \mathcal{J} = 1$, and various values $(\frac{\tilde{\mathcal{J}}}{\mathcal{J}}, \mu, \beta)$. In particular, as we vary (μ, β) we obtained the following results:

(i) When the temperature T is sufficiently large, there is a solution where $\frac{S_E}{\beta}$ is similar to the (annealed) free energy of two uncoupled SYK systems. We shall call this solution the two-black hole solution.

(ii) As we decrease the temperature slowly (we have chosen $\Delta T = 0.0001$), this solution is deformed continuously until some temperature $T = T_{c,2\mathrm{BH}}$. Once the temperature crosses $T_{c,2\mathrm{BH}}$, the two-black hole solution ceases to exist and the numerical analysis detects another solution where the free energy is almost constant in T. We shall call this solution the wormhole solution.

(iii) As we increase the temperature from $T < T_{c,2\mathrm{BH}}$ the wormhole solution is deformed continuously until some temperature $T = T_{c,\mathrm{WH}}$ which is greater than $T_{c,2\mathrm{BH}}$. Once T exceeds $T_{c,\mathrm{WH}}$ the wormhole solution disappears.

(iv) When μ is larger than some critical value μ_*, (ii) and (iii) do not occur; the two-black hole solution and the wormhole solution merge to a single solution that exists at any value of the temperature.

See figures 2 and 3. These behaviors of the solution and the free energy are qualitatively the same as those for the case with $\tilde{\mathcal{J}} = \mathcal{J}$ [31, 37]. In the temperature regime $T_{c,2\mathrm{BH}} <$

JHEP04(2023)145

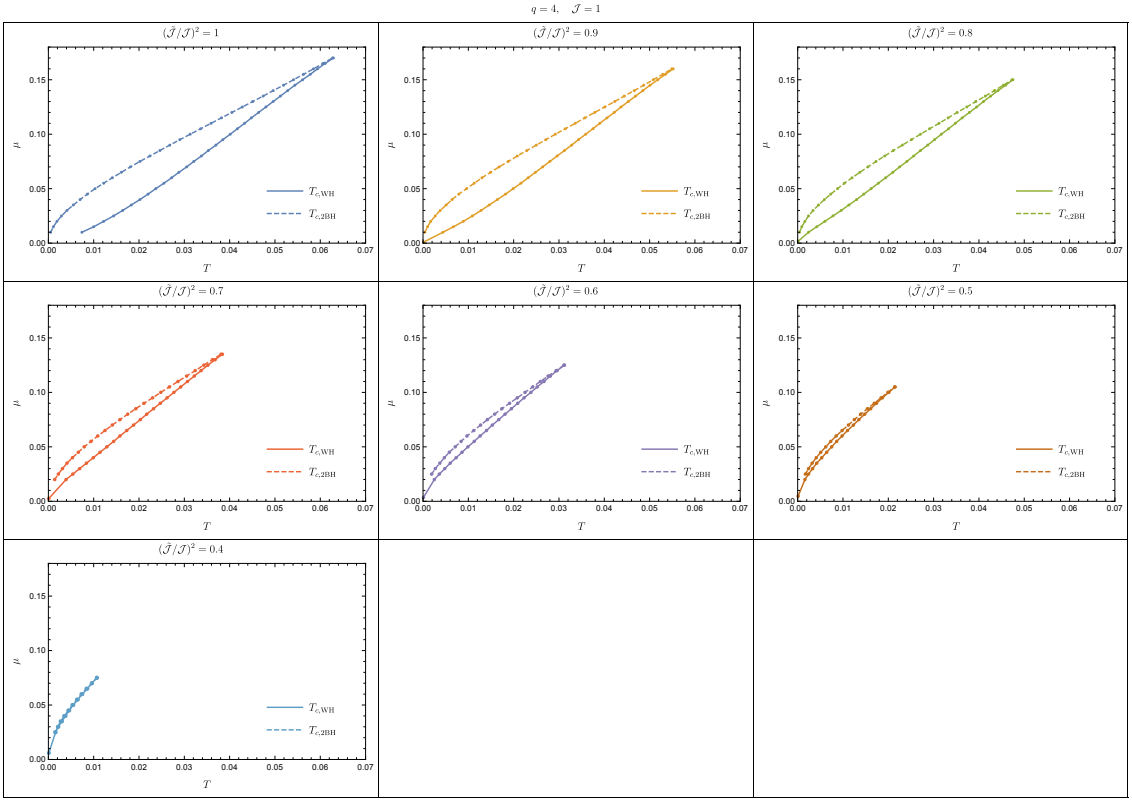

Figure 3. Phase diagram for various values of $\frac{\tilde{\mathcal{J}}}{\mathcal{J}}$. Points connected by the solid line are $T_{c,\mathrm{WH}}(\mu)$ such that the wormhole solution does not exists for $T > T_{c,\mathrm{WH}}(\mu)$. Points connected by the dashed line are $T_{c,\mathrm{2BH}}(\mu)$ such that the two-black hole solution does not exist for $T < T_{c,\mathrm{2BH}}(\mu)$. The two lines intersect at a point (μ_*, T_*) $(T_* = T_{c,\mathrm{WH}}(\mu_*) = T_{c,\mathrm{2BH}}(\mu_*))$ which depends on $\frac{\tilde{\mathcal{J}}}{\mathcal{J}}$. In the regime where either $\mu > \mu_*$ or $T > T_*$ is satisfied, the wormhole solution and the two-black hole solution are smoothly connected with each other.

$T < T_{c,\mathrm{WH}}$ both the two-black hole solution and the wormhole solution exist, hence the free energy is given by the smaller one of the two values of S_E evaluated at these two solutions. We observe that the two values cross at one point $T = T_c$, where the system undergoes a phase transition.

As we further vary $\frac{\tilde{\mathcal{J}}}{\mathcal{J}}$ we observed that these behaviors change in the following way:

(v) $T_{c,\mathrm{WH}}$ and T_c decrease as $\frac{\tilde{\mathcal{J}}}{\mathcal{J}}$ is decreased. On the other hand, $T_{c,\mathrm{2BH}}$ also decreases, but it is almost independent of $\frac{\tilde{\mathcal{J}}}{\mathcal{J}}$ when μ is small. This is consistent with the fact that $T_{c,\mathrm{2BH}}$ is determined as a property of the two-black hole solution where the off-diagonal component G_{LR}, Σ_{LR} are small and hence the correlation between $J^{(L)}_{i_1 i_2 \cdots i_q}$ and $J^{(R)}_{i_1 i_2 \cdots i_q}$ is less important. See figure 2.

(vi) The critical value μ_* of μ where the phase transition disappears decreases as $\frac{\tilde{\mathcal{J}}}{\mathcal{J}}$ is decreased. See figure 4. From the results, we also expect that μ_* becomes zero somewhere in the range $0.2 < \frac{\tilde{\mathcal{J}}^2}{\mathcal{J}^2} < 0.3$ (b and b'^2 in figure 4), that is, the phase transition completely disappears as $\frac{\tilde{\mathcal{J}}^2}{\mathcal{J}^2}$ is decreased below this value.

JHEP04(2023)145

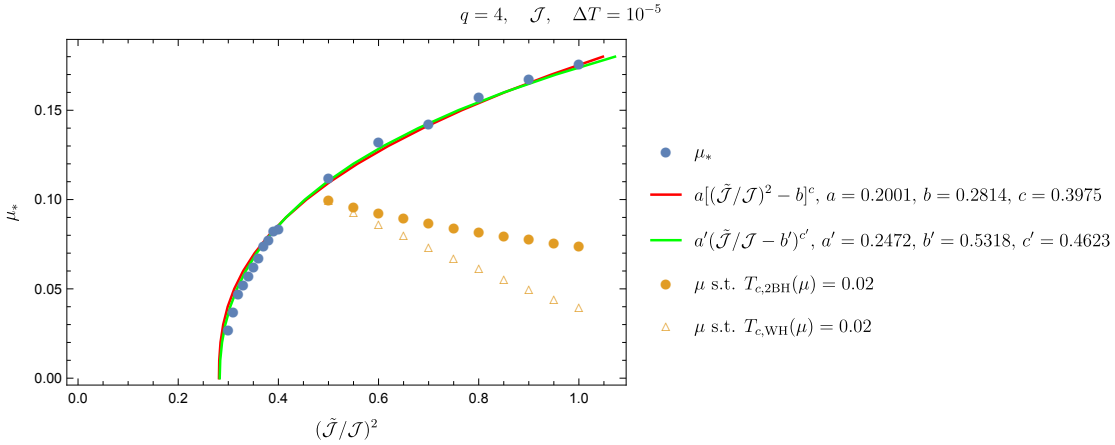

Figure 4. The critical value μ_* of μ for each $\frac{\tilde{\mathcal{J}}}{\mathcal{J}}$ such that the phase transition does not exist for $\mu > \mu_*$, with the red/green curve obtained by fitting the data with the ansatz $\mu_* = a\left(\left(\frac{\tilde{\mathcal{J}}}{\mathcal{J}}\right)^n - b\right)^c$. Here we have determined a, c by first fitting the data of $\frac{d\left(\left(\frac{\tilde{\mathcal{J}}}{\mathcal{J}}\right)^n\right)}{d\mu_*}$ obtained by the numerical differentiation with the ansatz $\log \frac{d\left(\left(\frac{\tilde{\mathcal{J}}}{\mathcal{J}}\right)^n\right)}{d\mu_*} = \left(\frac{1}{c} - 1\right)\log\frac{\mu_*}{a} + \log\frac{1}{ac}$ and then determined b by fitting $\left(\frac{\tilde{\mathcal{J}}}{\mathcal{J}}\right)^n$ with the ansatz $\left(\frac{\tilde{\mathcal{J}}}{\mathcal{J}}\right)^n = \left(\frac{\mu_*}{a}\right)^{\frac{1}{c}} + b$. We have performed the fitting for $n = 1, 2$ and have found almost the same value of $b^{\frac{1}{n}}$, the value of $\frac{\tilde{\mathcal{J}}}{\mathcal{J}}$ where μ_* vanishes. For comparison, we have also displayed the points on the phase transition lines in the $\left(\mu, \frac{\tilde{\mathcal{J}}^2}{\mathcal{J}^2}\right)$-plane with a fixed temperature $T = 0.02$, i.e., the points where $T_{c,\mathrm{2BH}}\left(\mu; \frac{\tilde{\mathcal{J}}^2}{\mathcal{J}^2}\right) = 0.02$ and $T_{c,\mathrm{WH}}\left(\mu; \frac{\tilde{\mathcal{J}}^2}{\mathcal{J}^2}\right) = 0.02$.

Though the observation that μ_c depends on $\frac{\tilde{\mathcal{J}}}{\mathcal{J}}$ might be surprising, it is consistent with the fact that for $\frac{\tilde{\mathcal{J}}}{\mathcal{J}} = 0$, our model (2.1) is equivalent in the large N limit to the single-side model [46] which does not exhibit phase transition at any value of μ [36].

Notice that our claim (vi) for the absence of the phase transition is based on the observation that S_E obtained by decreasing T from a high-temperature regime and S_E obtained by increasing T from a low -temperature regime do not deviate at discrete points spaced with $\Delta T = 0.00001$, but this does not exclude the possibility that the phase transition exists with $T_{c,\mathrm{WH}} - T_{c,\mathrm{2BH}} < 0.00001$. In our approach, it is in principle impossible to *prove* the absence of phase transition at $\mu > \mu_*$. As we see in section 4, however, we can rigorously show the absence of the phase transition in the large q limit.

3.2 Energy gap

Next, we look at the energy gap E_{gap} of the two-coupled model (2.1) in the large N limit. In [36] we have observed that E_{gap} of the model (2.1) with $\tilde{\mathcal{J}} = \mathcal{J}$ [31] and E_{gap} of the single-sided model [46] which is equivalent in the large N limit to the two-coupled model with $\tilde{\mathcal{J}} = 0$ show different power law behavior for small μ: $E_{\mathrm{gap}}(\tilde{\mathcal{J}} = \mathcal{J}) \sim \mu^{\frac{q}{2(q-1)}}$ and $E_{\mathrm{gap}}(\tilde{\mathcal{J}} = 0) \sim \mu^{\frac{q}{q-2}}$. In this section, we investigate how these two behaviors are interpolated as we vary $\frac{\tilde{\mathcal{J}}}{\mathcal{J}}$ from 0 to 1.

JHEP04(2023)145

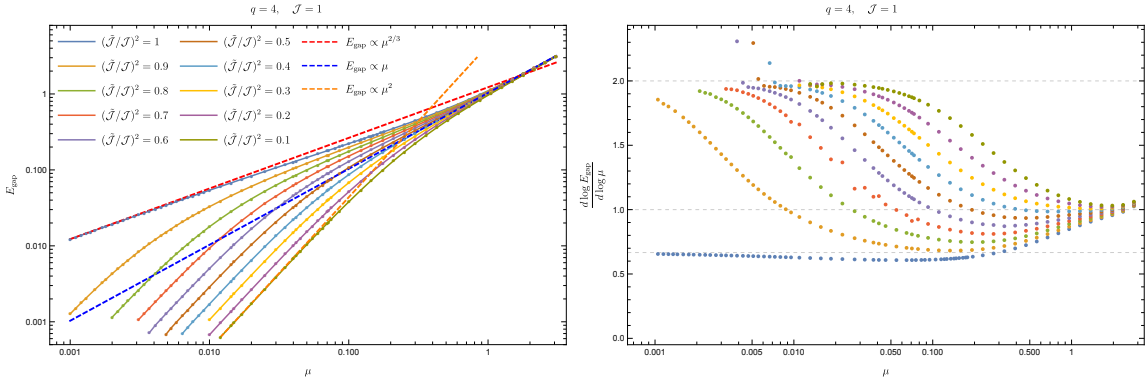

Figure 5. The energy gap $E_{\rm gap}$ for various values of $\frac{\tilde{\mathcal{J}}}{\mathcal{J}}$ read off by fitting $G_{ab}(\tau)$ with the ansatzes (3.4). Here the legends of the right plot are the same as those indicated in the left plot.

The large N energy gap can be read off from the Euclidean two-point functions $G_{ab}(\tau)$ in the low-temperature phase as [31]

$$G_{LL}(\tau) \sim \cosh\Big[E_{\rm gap}\Big(\frac{\beta}{2}-\tau\Big)\Big], \quad G_{LR}(\tau) \sim \sinh\Big[E_{\rm gap}\Big(\frac{\beta}{2}-\tau\Big)\Big]. \qquad (1 \ll \tau \ll \beta) \quad (3.4)$$

By fitting $G_{ab}(\tau)$ with these ansatz we have obtained $E_{\rm gap}$ for $0.1 \leq \frac{\tilde{\mathcal{J}}^2}{\mathcal{J}^2} \leq 1$ as displayed in figure 5. We observe the followings

- For any value of μ, $E_{\rm gap}$ increases monotonically in $\frac{\tilde{\mathcal{J}}^2}{\mathcal{J}^2}$.
- When μ is sufficiently large, $E_{\rm gap}$ scales as $E_{\rm gap} \sim \mu$ regardless of the value of $\frac{\tilde{\mathcal{J}}^2}{\mathcal{J}^2}$.
- When μ is sufficiently small, $E_{\rm gap} \sim \mu^{2/3}$ for $\frac{\tilde{\mathcal{J}}^2}{\mathcal{J}^2} = 1$ while $E_{\rm gap} \sim \mu^2$ for $\frac{\tilde{\mathcal{J}}^2}{\mathcal{J}^2} < 1$.
- When $\frac{\tilde{\mathcal{J}}^2}{\mathcal{J}^2}$ is less than 1 but close to 1, there is also an intermediate regime where $E_{\rm gap} \sim \mu^{\frac{2}{3}}$. The range of the intermediate regime becomes wider in μ as $\frac{\tilde{\mathcal{J}}^2}{\mathcal{J}^2}$ approaches 1.

3.3 Real time response

Next, we study real-time dynamics of the two-coupled model (2.3), in particular, the transmission amplitude T_{LR} [47] which measures how an excitation on the right side affects the left side at a late time, and the decay of the out-of-time-ordered four-point function [48] which is characterized with the quantum chaos exponent λ_L. For this purpose, we need to continue the $G\Sigma$ formalism for real τ (2.7)–(2.9) in section 2 to complex $u = \tau + it$, which can be done in the following way.[5] First, we define the two different components of the two point functions at $\mathrm{Re}[u] = 0$, $G^{>}_{ab}, G^{<}_{ab}$, depending on how $\mathrm{Re}[u]$ approaches 0:

$$\begin{aligned} G^{>}_{ab}(t_1,t_2) &= -iG_{ab}(it_1^-, it_2^+) = -i\lim_{\epsilon\to+0} G_{ab}(\epsilon+it_1, -\epsilon+it_2), \\ G^{<}_{ab}(t_1,t_2) &= -iG_{ab}(it_1^+, it_2^-) = -i\lim_{\epsilon\to+0} G_{ab}(-\epsilon+it_1, \epsilon+it_2), \end{aligned} \qquad (3.5)$$

[5]Note the calculations in this section are completely parallel to the case with $J^{(L)}_{i_1\cdots i_q} = J^{(R)}_{i_1\cdots i_q}$ in [37]. Hence we shall skip the details of the derivations which can be found in section 3 in [37].

JHEP04(2023)145

with which we also define the retarded/advanced components of the two-point functions as

$$G^R_{ab}(t_1,t_2) = \theta(t_1-t_2)(G^>(t_1,t_2) - G^<(t_1,t_2)),$$
$$G^A_{ab}(t_1,t_2) = \theta(t_2-t_1)(G^<(t_1,t_2) - G^>(t_1,t_2)). \tag{3.6}$$

We also define the $>, <, R, A$ components of $\Sigma_{ab}(u)$ at $u = it$ in the same ways.

With these notations, the real-time continuation of the Schwinger-Dyson equations (2.9) reduce to the followings

$$\widetilde{G}^R_{LL}(\omega) = \frac{-(-\omega + \widetilde{\Sigma}^R_{RR}(\omega))}{(-\omega+\widetilde{\Sigma}^R_{LL}(\omega))(-\omega+\widetilde{\Sigma}^R_{RR}(\omega)) - (\widetilde{\Sigma}^R_{LR}+i\mu)(\widetilde{\Sigma}^R_{RL}-i\mu)},$$
$$\widetilde{G}^R_{LR}(\omega) = \frac{\widetilde{\Sigma}^R_{LR}(\omega) + i\mu}{(-\omega+\widetilde{\Sigma}^R_{LL}(\omega))(-\omega+\widetilde{\Sigma}^R_{RR}(\omega)) - (\widetilde{\Sigma}^R_{LR}+i\mu)(\widetilde{\Sigma}^R_{RL}-i\mu)},$$
$$\widetilde{G}^R_{RL}(\omega) = \frac{\widetilde{\Sigma}^R_{RL}(\omega) - i\mu}{(-\omega+\widetilde{\Sigma}^R_{LL}(\omega))(-\omega+\widetilde{\Sigma}^R_{RR}(\omega)) - (\widetilde{\Sigma}^R_{LR}+i\mu)(\widetilde{\Sigma}^R_{RL}-i\mu)},$$
$$\widetilde{G}^R_{RR}(\omega) = \frac{-(-\omega + \widetilde{\Sigma}^R_{LL}(\omega))}{(-\omega+\widetilde{\Sigma}^R_{LL}(\omega))(-\omega+\widetilde{\Sigma}^R_{RR}(\omega)) - (\widetilde{\Sigma}^R_{LR}+i\mu)(\widetilde{\Sigma}^R_{RL}-i\mu)},$$
$$\Sigma^>_{ab}(t_1,t_2) = -\frac{i^q\mathcal{J}^2_{ab}}{q} s_{ab} G^>_{ab}(t_1,t_2)^{q-1}, \tag{3.7}$$
$$\Sigma^R_{ab}(t_1,t_2) = \theta(t_1-t_2)(\Sigma^>_{ab}(t_1,t_2) + \Sigma^>_{ba}(t_2,t_1)),$$
$$\widetilde{G}^>_{ab}(\omega) = \frac{\widetilde{G}^R_{ab}(\omega) - (\widetilde{G}^R_{ba}(\omega))^*}{1+e^{-\beta\omega}}, \tag{3.8}$$

where we have defined the Fourier transform in the real time t as

$$\widetilde{f}^X(\omega) = \int_{-\infty}^{\infty} dt e^{i\omega t} f^X(t), \quad f^X(t) = \int_{-\infty}^{\infty} \frac{d\omega}{2\pi} e^{-i\omega t}\widetilde{f}^X(t), \quad (f = G_{ab}, \Sigma_{ab}, \quad X = >, <, R, A). \tag{3.9}$$

Note that we can obtain $G_{ab}(u)$ for general $u \in \mathbb{C}$ from $\widetilde{G}^R_{ab}(\omega)$ as

$$G_{ab}(u) = iG^>_{ab}(t=-iu) = i\int \frac{d\omega}{2\pi} e^{-\omega u} \frac{\widetilde{G}^R_{ab}(\omega) - (\widetilde{G}^R_{ba}(\omega))^*}{1+e^{-\beta\omega}}, \tag{3.10}$$

which we use to compute the chaos exponent in section 3.3.2.

3.3.1 Transmission amplitude in low temperature regime

Let us define the transmission amplitude $T_{LR}(t)$ as $T_{LR}(t) = 2|G^>_{LR}(t)|$, which measures the probability to find the excitation of ψ^L_i at time t after the insertion of ψ^R_i at time $t = 0$ [47]. We have displayed $T_{LR}(t)$ for $q = 4, \mathcal{J} = 1, \mu = 0.1, T = 0.019$, and various values of $\frac{\tilde{\mathcal{J}}^2}{\mathcal{J}^2}$ in figure 6. We find that the transmission is reduced by decreasing LR correlation $\frac{\tilde{\mathcal{J}}^2}{\mathcal{J}^2}$. Note that when the temperature is sufficiently small, $G^>_{LR}(t)$ is well approximated by a single quasi-particle with the speed ω_1 and a finite lifetime Γ_1: $G^>_{LR}(t) \sim e^{-i\omega_1 t - \Gamma_1 t}$. Hence the suppression of $T_{LR}(t)$ can be explained by the decrease of ω_1 and increase of Γ_1, both of which are encoded in the first peak of the spectral function $\rho_{LR}(\omega) = -2\mathrm{Re}[\widetilde{G}_{LR}(\omega)]$, as $\frac{\tilde{\mathcal{J}}^2}{\mathcal{J}^2}$ is decreased. See figure 7.

JHEP04(2023)145

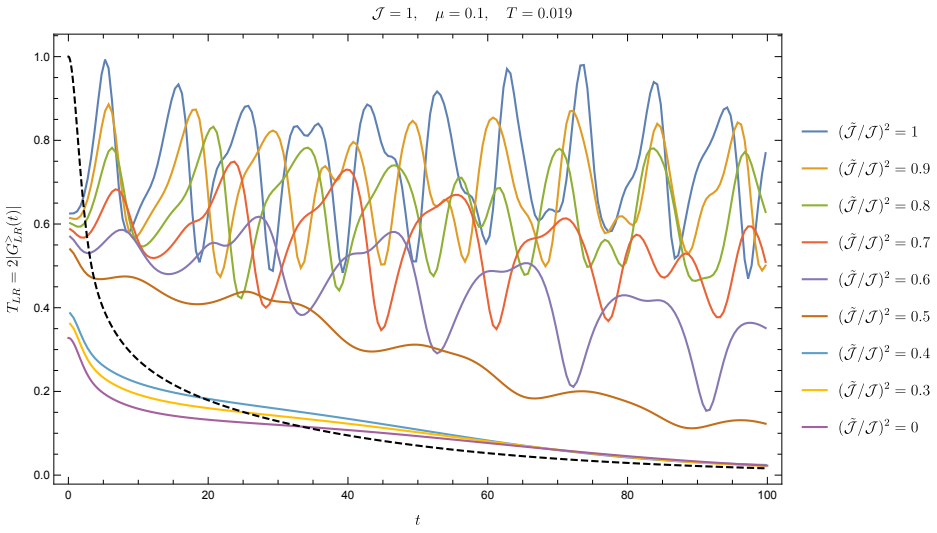

Figure 6. Transmission amplitude $T_{LR}(t) = 2|G^{>}_{LR}(t)|$ for various values of $\frac{\tilde{\mathcal{J}}^2}{\mathcal{J}^2}$ in the low-temperature phase. Note that for $\frac{\tilde{\mathcal{J}}^2}{\mathcal{J}^2} = 0.4$, there is no phase transition for $\mu = 0.1$ (see figure 3), hence $(\mu, T) = (0.1, 0.019)$ belongs to the supercritical regime. For comparison, we have also plotted $2|G^{>}(t)|$ for the single SYK model (dashed black line).

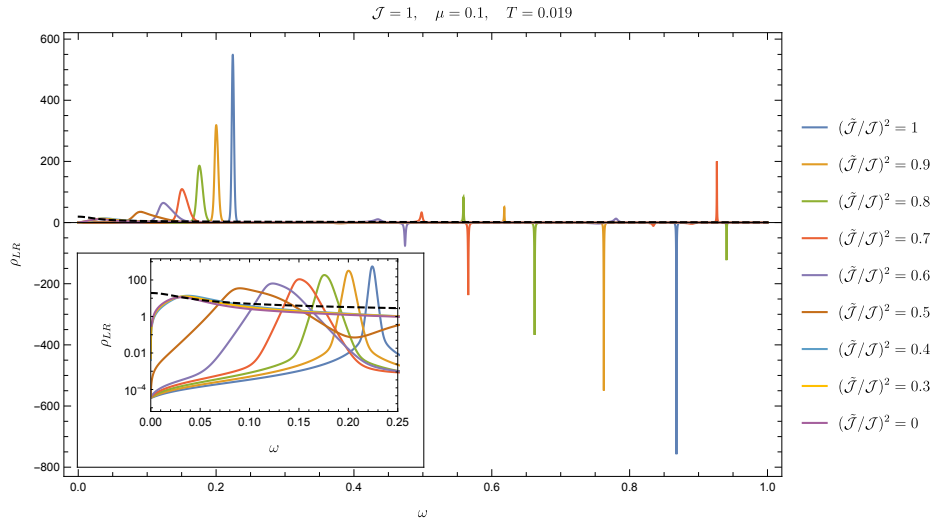

Figure 7. Spectral function $\rho_{LR}(\omega) = -2\mathrm{Re}[\widetilde{G}^{R}_{LR}(\omega)]$.

3.3.2 Chaos exponent

To compute the chaos exponent, we consider the four-point functions

$$\frac{1}{N^2}\sum_{i,j}^{N}\langle\psi_i^a(u_1)\psi_i^b(u_2)\psi_j^c(u_3)\psi_j^d(u_4)\rangle = \frac{1}{Z}\int \mathcal{D}G_{ab}\mathcal{D}\Sigma_{ab}G_{ab}(u_1,u_2)G_{cd}(u_1,u_2)e^{-NS}. \quad (3.11)$$

JHEP04(2023)145

with $u_1 = \frac{3\beta}{4} + it_1$, $u_2 = \frac{\beta}{4} + it_2$, $u_3 = \frac{\beta}{2}$, $u_4 = 0$. The chaos exponent λ_L is given by the following late-time behavior of the four-point functions:

$$\frac{1}{N^2}\sum_{i,j}^{N}\langle\psi_i^a(u_1)\psi_i^b(u_2)\psi_j^c(u_3)\psi_j^d(u_4)\rangle = G_{ab}(u_1,u_2)G_{cd}(u_3,u_4) + \frac{1}{N}\mathcal{F}_{abcd}(u_1,u_2,u_3,u_4),$$
$$\mathcal{F}_{abcd}(u_1,u_2,u_3,u_4) \sim e^{\frac{\lambda_L(t_1+t_2)}{2}} \quad (t_1,t_2 \gg 1). \tag{3.12}$$

In the large N limit and at late times, we find that $\mathcal{F}_{abcd}(t_1,t_2)$ obeys the following equation [37]

$$\mathcal{F}_{abcd}(t_1,t_2) \approx \sum_{ef}\int dtdt' \mathcal{K}^R_{abef}(t_1,t_2,t,t')\mathcal{F}_{efcd}(t,t'),$$
$$\mathcal{K}^R_{abcd}(t_1,t_2,t_3,t_4) = -\frac{\mathcal{J}_{cd}^2 2^{q-1}(q-1)}{q}G^R_{ac}(t_1-t_3)G^R_{bd}(t_2-t_4)s_{cd}G_{cd}\left(\frac{\beta}{2}+i(t_3-t_4)\right)^{q-2}. \tag{3.13}$$

If we substitute the ansatz $\mathcal{F}_{abcd}(t_1,t_2) = e^{\frac{\lambda_L(t_1+t_2)}{2}} f_{abcd}(t_{12})$, this equation can be rewritten as an eigenequation of $f_{ab\cdot\cdot}(t)$ with eingenvalue 1 [37]:

$$\sum_{e,f}\int dt' \mathcal{M}_{abef}(\lambda_L;t,t')f_{efcd}(t') \approx f_{abcd}(t),$$
$$\mathcal{M}_{abcd}(\lambda_L;t,t') = -\frac{\mathcal{J}_{cd}^2 2^{q-1}(q-1)}{q}e^{-\frac{\lambda_L(t-t')}{2}}$$
$$\times\left[\int dt'' G^R_{ac}(t-t'-t'')G^R_{bd}(-t'')e^{\lambda_L t''}\right]s_{cd}G_{cd}\left(\frac{\beta}{2}+it'\right)^{q-2}. \tag{3.14}$$

The chaos exponent λ_L can be determined so that the largest eigenvalue of the λ_L-dependent kernel $\mathcal{M}_{abcd}(\lambda_L;t,t')$ crosses 1.

Notice that (3.14) can be decomposed into the following two equations with $\sigma = \pm 1$ [37]

$$\begin{pmatrix} f_{2,LL}(t) + \sigma f_{2,RR}(t) \\ f_{2,LR}(t) - \sigma f_{2,RL}(t)\end{pmatrix}_a = \sum_b \int dt' \mathcal{M}_{ab}(\sigma,\lambda_L;t,t')\begin{pmatrix} f_{2,LL}(t') + \sigma f_{2,RR}(t') \\ f_{2,LR}(t') - \sigma f_{2,RL}(t')\end{pmatrix}_b, \tag{3.15}$$

where $a,b = 1,2$ and

$$\mathcal{M}_{ab}(\sigma,\lambda_L;t,t')$$
$$= \begin{pmatrix} (M_{1,LLLL}(t-t') + \sigma M_{1,LRLR}(t-t'))M_{2,LL}(t') & (M_{1,LLLR}(t-t') - \sigma M_{1,LRLL}(t-t'))M_{2,LL}(t') \\ -(M_{1,LLLR}(t-t') - \sigma M_{1,LRLL}(t-t'))M_{2,LR}(t') & (M_{1,LLLL}(t-t') + \sigma M_{1,LRLR}(t-t'))M_{2,LR}(t')\end{pmatrix}, \tag{3.16}$$

with

$$f_{2,ab}(t_{12}) = e^{\frac{\lambda_L t_{12}}{2}} f_{ab}(t_{12}),$$
$$M_{1,abcd}(t) = \int dt' G^R_{ab}(t-t')G^R_{cd}(-t')e^{\lambda_L t'},$$
$$M_{2,ab}(t) = -\frac{\mathcal{J}_{ab}^2 2^{q-1}(q-1)}{q}s_{ab}G_{ab}\left(\frac{\beta}{2}+it\right)^{q-2}. \tag{3.17}$$

JHEP04(2023)145

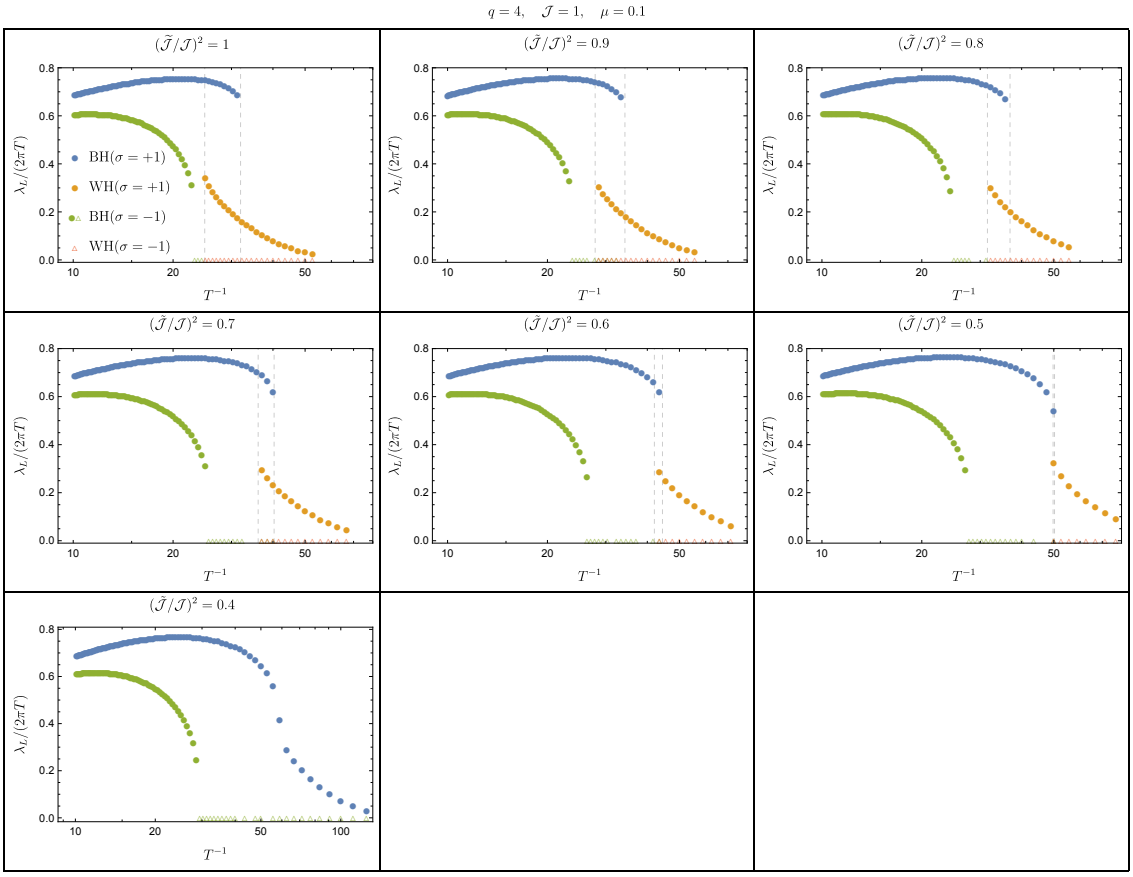

Figure 8. The chaos exponent λ_L for the two sectors $\sigma = \pm 1$. Here we have displayed the data points where the largest absolute value of the eigenvalues of $\mathcal{M}_{ab}(-1, \lambda_L; t, t')$ does not cross 1 in $0 < \lambda_L \leq 2\pi T$ with empty triangle markers.

Hence we can compute the chaos exponent $\lambda_L(\sigma)$ for each sector rather than computing only the chaos exponent of the full system $\lambda_L = \max\{\lambda_L(1), \lambda_L(-1)\}$.

By performing a binary search for the value of λ_L in the range $0 < \lambda_L \leq 2\pi T$ such that the largest eigenvalue of $\mathcal{M}_{ab}(\sigma, \lambda_L; t, t')$ is 1, we obtained the chaos exponent for $\sigma = \pm 1$ and various values of $\frac{\tilde{\mathcal{J}}^2}{\mathcal{J}^2}$, as displayed in figure 8. We found that as $\frac{\tilde{\mathcal{J}}^2}{\mathcal{J}^2}$ is decreased the chaos exponent of each sector increases while their temperature dependence remains qualitatively the same. This result may be interpreted in the following way. Let us assume that the chaos exponent is associated with the operator growth over a single side (say Left). In the two-coupled system, the operator growth on a single side should be reduced due to the leakage of the operator to the operators supported on the other side. As we have seen in the previous section, as $\frac{\tilde{\mathcal{J}}^2}{\mathcal{J}^2}$ is decreased the LR transmission becomes suppressed. Hence the chaos exponent is expected to become larger as $\frac{\tilde{\mathcal{J}}^2}{\mathcal{J}^2}$ is decreased, which is consistent with the results in figure 8. Note, however, that this interpretation is only a matter of speculation at present. In terms of the operator growth, the growth over the L side and the "leakage" would be characterized respectively by the commutator squares $\sum_{i,j}\langle -\{\psi_i^L(t), \psi_j^L(0)\}^2\rangle$ and $\sum_{i,j}\langle -\{\psi_i^L(t), \psi_j^R(0)\}^2\rangle$, and the relevant components

JHEP04(2023)145

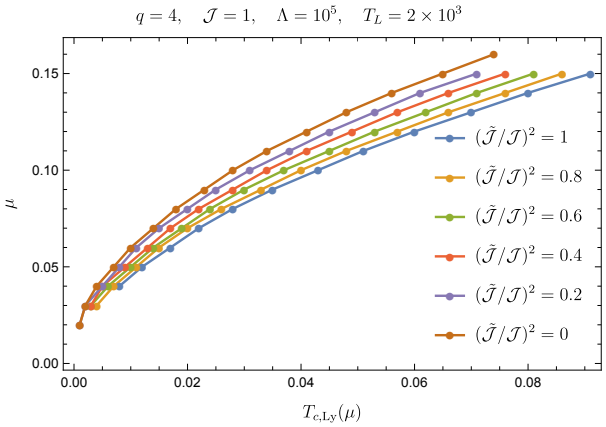

Figure 9. The temperature $T_{c,\mathrm{Ly}}$ where the binary search to determine $\lambda_L(-1)$ fails.

of the regularized out-of-time-ordered correlators are respectively $\mathcal{F}_{LLLL}$ and $\mathcal{F}_{RRLL}$. Since the ladder kernel mixes these two components, we are not able to evaluate the two effects separately with the method in this section. It would be interesting for future work to analyze the operator growth of the two-coupled model directly, keeping track of the size as an operator on the L-side and the size as an operator on the R-side, not only the total size. Such analysis might provide us with a more concrete picture of the relation between the scrambling property of the system and the uncorrelated disorder.

Interestingly we also found that when the temperature is lower than some critical value $T_{c,\mathrm{Ly}}(\frac{\tilde{\mathcal{J}}}{\mathcal{J}}, \mu)$ (which is larger than $T_{c,\mathrm{2BH}}$), the absolute values of the eigenvalues of $\mathcal{M}_{ab}(-1, \lambda_L; t, t')$ are smaller than 1 for any value of λ_L in $0 < \lambda_L \leq 2\pi T$. This would imply that there are no exponentially growing modes in $\sigma = -1$ sector for $T < T_{c,\mathrm{Ly}}$. In figure 9 we display the observed values of $T_{c,\mathrm{Ly}}$ for various $\tilde{\mathcal{J}}/\mathcal{J}$ and μ.

4 large q limit

In the large q limit, we can study the $J^{(L)}_{i_1\cdots i_q} \neq J^{(R)}_{i_1\cdots i_q}$ model analytically. In this section, we study this limit and compare it with the results of the numerical analysis at finite q in the previous section.

4.1 Large q limit at zero temperature

In the large q limit, the $G\Sigma$ action reduces to the Liouville action:

$$\frac{S_E}{N} = \frac{1}{8q^2}\int d\tau_1 \int d\tau_2 \Big(\partial_{\tau_1} g_{LL}(\tau_1,\tau_2)\partial_{\tau_2} g_{LL}(\tau_1,\tau_2) - \partial_{\tau_1} g_{LR}(\tau_1,\tau_2)\partial_{\tau_2} g_{LR}(\tau_1,\tau_2)\Big)$$
$$- \frac{\mathcal{J}^2}{2q^2}\int d\tau_1 \int d\tau_2 e^{g_{LL}(\tau_1,\tau_2)} - \frac{\tilde{\mathcal{J}}^2}{2q^2}\int d\tau_1 \int d\tau_2 e^{g_{LR}(\tau_1,\tau_2)} - \frac{\hat{\mu}}{2q^2}\int d\tau g_{LR}(\tau,\tau), \quad (4.1)$$

with the following ansatz for the large q expansion

$$G_{LL}(\tau) = G_{RR}(\tau) = \frac{1}{2}\mathrm{sgn}(\tau)\Big(1 + \frac{1}{q} g_{LL}(\tau) + \cdots\Big),$$
$$G_{LR}(\tau) = -G_{RL}(\tau) = \frac{i}{2}\Big(1 + \frac{1}{q} g_{LR}(\tau) + \cdots\Big). \quad (4.2)$$

JHEP04(2023)145

Here we have also scaled μ so that $\hat{\mu} = \mu q$ is kept finite in the large q limit. At a small temperature and a late time of order $\tau \sim q$, this approximation is not valid because of the exponential decay of the correlation functions. In this case, we also consider the solution in $\tau \gg q$ regime and impose the matching condition between $\tau \ll q$ and $\tau \gg q$ solutions, as we discuss in section 4.2. The Schwinger-Dyson equations reduce to the following two equations:

$$\begin{aligned} \partial_\tau^2 g_{LL}(\tau) &= 2\mathcal{J}^2 e^{g_{LL}(\tau)}, \qquad (\text{for} \quad \tau > 0) \\ \partial_\tau^2 g_{LR}(\tau) &= -2\tilde{\mathcal{J}}^2 e^{g_{LR}(\tau)} - 2\hat{\mu}\delta(\tau), \end{aligned} \tag{4.3}$$

with the boundary conditions

$$\begin{aligned} g_{LL}(0) = 0, \qquad \partial_\tau g_{LR}(0^+) = -\hat{\mu}, \\ g_{LL}(\tau) - g_{LR}(\tau) \to 0, \qquad \text{as} \quad \tau \to \infty. \end{aligned} \tag{4.4}$$

The general solution of the equations (4.3) is

$$\begin{aligned} e^{g_{LL}(\tau)} &= \frac{\alpha^2}{\mathcal{J}^2 \sinh^2(\alpha|\tau| + \gamma)}, \\ e^{g_{LR}(\tau)} &= \frac{\tilde{\alpha}^2}{\tilde{\mathcal{J}}^2 \cosh^2(\tilde{\alpha}|\tau| + \tilde{\gamma})}, \end{aligned} \tag{4.5}$$

with constants of the integration $\alpha, \tilde{\alpha}, \gamma, \tilde{\gamma}$. These parameters are determined by the boundary conditions which depend on the temperature.

Each of the boundary conditions (4.4) fixes the constants of integration in the following way. First, the boundary conditions at $\tau = 0$ give the relations

$$\begin{aligned} g_{LL}(0) = 0 \quad &\Rightarrow \quad \frac{\alpha}{\mathcal{J}\sinh\gamma} = 1, \\ \partial_\tau g_{LR}(0^+) = -\hat{\mu} \quad &\Rightarrow \quad 2\tilde{\alpha}\tanh\tilde{\gamma} = \hat{\mu}, \end{aligned} \tag{4.6}$$

whereas the boundary condition at $\tau = \infty$ gives

$$g_{LL}(\tau) - g_{LR}(\tau) \to 0, \qquad \text{as} \quad \tau \to \infty \qquad \Rightarrow \qquad \tilde{\gamma} = \gamma + s, \qquad \alpha = \tilde{\alpha}. \tag{4.7}$$

Here $s = \log \frac{\mathcal{J}}{\tilde{\mathcal{J}}}$ is a positive parameter and vanishes when $\tilde{\mathcal{J}} = \mathcal{J}$. Finally, γ satisfies the equation

$$\sinh\gamma \tanh(\gamma + s) = \frac{\hat{\mu}}{2\mathcal{J}}, \tag{4.8}$$

and other parameters are determined through γ. The physical gap E_{gap} is given by

$$E_{\text{gap}} = \frac{2\alpha}{q}. \tag{4.9}$$

For the small $j \equiv \mathcal{J} - \tilde{\mathcal{J}}$ limit, we can separate the scale of Maldacena-Qi behavior and Kourkoulou-Maldacena behavior. When $j \ll \mu$, we can ignore the parameter s and we obtain

$$\sinh\gamma\tanh\gamma = \frac{\hat{\mu}}{2\mathcal{J}}, \tag{4.10}$$

JHEP04(2023)145

which is exactly the same equation as in the Maldacena-Qi model. γ is given by

$$\tanh^2\gamma = \frac{\epsilon}{2}\left(\sqrt{4+\epsilon^2}-\epsilon\right), \qquad \epsilon = \frac{\hat{\mu}}{2\mathcal{J}}. \tag{4.11}$$

In the range $j \ll \hat{\mu} \ll \mathcal{J}$, we can expand as

$$\gamma \approx \sqrt{\epsilon} = \sqrt{\frac{\hat{\mu}}{2\mathcal{J}}}, \qquad \alpha = \mathcal{J}\sinh\gamma \approx \sqrt{\frac{\hat{\mu}\mathcal{J}}{2}}, \tag{4.12}$$

and the gap is given by

$$E_{\text{gap}} = \frac{2\alpha}{q} \approx \frac{\sqrt{2\hat{\mu}\mathcal{J}}}{q}. \tag{4.13}$$

This parameter regime exists only when $j \ll \mathcal{J}$. In the regime $\hat{\mu} \ll j$, we can ignore γ from the term $\tanh(\gamma+s)$. Therefore we obtain the equation

$$\sinh\gamma\tanh s \approx \frac{\hat{\mu}}{2\mathcal{J}}. \tag{4.14}$$

We can evaluate $\tanh s$ as

$$\tanh s = \frac{e^s - e^{-s}}{e^s + e^{-s}} = \frac{\mathcal{J}^2 - \tilde{\mathcal{J}}^2}{\mathcal{J}^2 + \tilde{\mathcal{J}}^2}. \tag{4.15}$$

Then, γ is evaluated as

$$\sinh\gamma \approx \frac{\hat{\mu}}{2\mathcal{J}\tanh s}. \tag{4.16}$$

When $\tilde{\mathcal{J}} = 0$ this reduces to the relation of Kourkoulou-Maldacena model. This parameter regime always exists but we need to take $\hat{\mu}$ to be smaller than j. When $\tilde{\mathcal{J}} = \mathcal{J}$, i.e., the perfect correlation between left and right SYK model, this regime disappears, which occurs in the Maldacena-Qi model. The parameter α becomes $\alpha \approx \frac{\hat{\mu}}{2\tanh s}$. The mass gap in this limit becomes

$$E_{\text{gap}} = \frac{2\alpha}{q} \approx \frac{\hat{\mu}}{q\tanh s}. \tag{4.17}$$

For $j = \mathcal{J}$, i.e., when there are no correlations between $J^{(L)}_{i_1\cdots i_q}$ and $J^{(R)}_{i_1\cdots i_q}$, we have $E_{\text{gap}} = \frac{\hat{\mu}}{q}$, which is the same as that of the Kourkoulou-Maldacena model.

Let us study how the behavior of E_{gap} in μ changes when we decrease μ. The plot of E_{gap} as a function of μ is shown in figure 10. The power of the gap in μ is defined as $\frac{d\log E_{\text{gap}}}{d\log\mu}$. Here we take the derivative with respect to μ while we fix $\mathcal{J}$ and $\tilde{\mathcal{J}}$. Then s is also fixed and this is equivalent to taking the derivative with respect to γ while fixing s. This becomes

$$\frac{d\log E_{\text{gap}}}{d\log\mu} = \frac{\hat{\mu}}{\alpha}\frac{\partial\gamma}{\partial\hat{\mu}}\frac{\partial\alpha}{\partial\gamma} = \frac{\sinh(\gamma+s)\cosh(\gamma+s)}{\sinh(\gamma+s)\cosh(\gamma+s)+\tanh\gamma}. \tag{4.18}$$

The plot of (4.18) is shown in figure 11. We can see that for a very small j, there is a region where the power in μ is almost $1/2$, which is the behavior in the Maldacena-Qi model. On the other hand, even for small j, the power in μ approaches 1 for sufficiently small μ as we expect.

JHEP04(2023)145

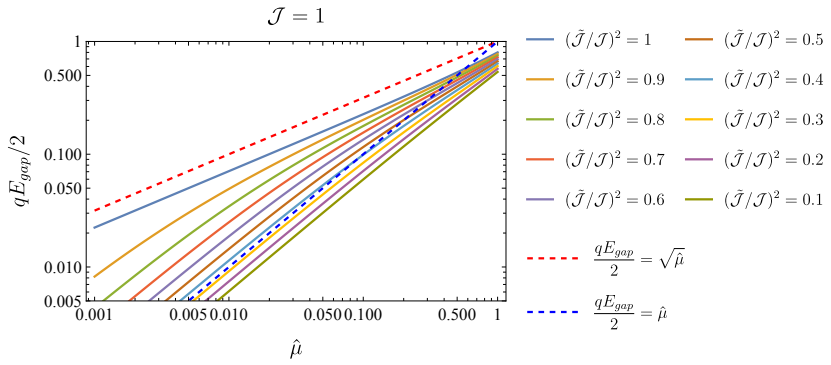

Figure 10. Plot of E_{gap} as a function of $\hat{\mu}$.

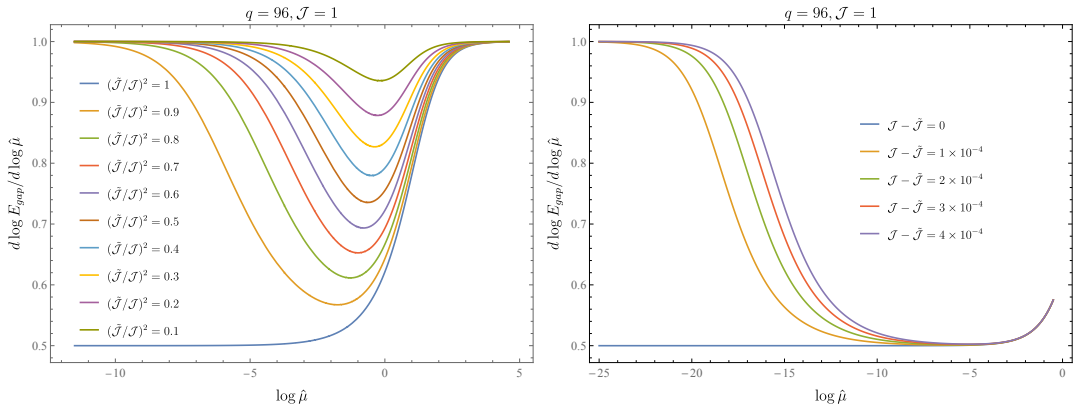

Figure 11. Plots of the power of E_{gap} in $\hat{\mu}$.

The real-time correlation function is obtained by analytically continuing to the Lorentzian time. At a low temperature of order $\beta = O(q \log q)$ we see that there are no decay and the return amplitude just oscillates. This is because the decay rate is of order $e^{-(\frac{q}{2}-1)E_{\text{gap}}}$, which is non-perturbatively small in q [37, 49] at large q limit, and we did not take into account this decay rate at large q. Since the decay rate is also suppressed by the energy gap E_{gap}, the decay rate will increase as we decrease the correlation of the random couplings between the two sides.

4.2 Finite temperature

For $\tau \ll q$ we can still use the solution (4.5) together with the boundary conditions at $\tau \to 0$ (4.6). For $\tau \gg q$, we can make a different approximation for the Schwinger-Dyson equation (2.13) which goes as follows. First, from the second equation in (2.9) we can approximate the self energy $\Sigma_{ab}(\tau)$ at the time scale of $G_{ab}(\tau)$ by the delta function configurations (see section 5.4 in [31])

$$\Sigma_{LL}(\tau), \Sigma_{RR}(\tau) \approx \rho \partial_\tau \delta(\tau), \quad \Sigma_{LR}(\tau) = -\Sigma_{RL}(\tau) \approx -i\nu\delta(\tau), \quad \nu = i\int_0^\beta \Sigma_{LR}(\tau)d\tau = \frac{2\tilde{\alpha}}{q}, \tag{4.19}$$

JHEP04(2023)145

where ρ is a constant of order $\mathcal{O}(q^{-1})$. We have evaluated the last integration by using $G_{LR}(\tau)$ in the small τ regime (4.2), (4.5) which gives $i\Sigma_{LR}(\tau) \approx \frac{\tilde{\alpha}^2}{q\cosh^2(\tilde{\alpha}|\tau|+\tilde{\gamma})} + \mu\delta(\tau)$, and replacing the domain of integration with $(-\infty, \infty)$. With (4.19), the other Schwinger-Dyson equations are simplified as

$$(1-\rho)\partial_\tau G_{LL}(\tau) - i\nu G_{LR}(\tau) = 0, \tag{4.20}$$
$$(1-\rho)\partial_\tau G_{LR}(\tau) + i\nu G_{LL}(\tau) = 0. \tag{4.21}$$

We can ignore ρ in each equation since it gives a sub-leading correction in the large q limit. Solving these equations we have

$$G_{LL}(\tau) = A\cosh\left[\nu\left(\frac{\beta}{2}-\tau\right)\right], \qquad G_{LR}(\tau) = iA\sinh\left[\nu\left(\frac{\beta}{2}-\tau\right)\right], \tag{4.22}$$

where A is an integration constant. The other integration constant (translation in τ) is fixed by the conditions $G_{LL}(\tau) = G_{LL}(\beta-\tau), G_{LR}(\tau) = -G_{LR}(\beta-\tau)$ which follows from (2.14).

Let us define $\sigma = qe^{-\beta\nu}$ as a new parameter corresponding to the temperature, and assume that σ is of order $\mathcal{O}(q^0)$ (i.e., $\beta = \mathcal{O}(q\log q)$). Matching the two solutions in the overlapping regime, i.e., the large τ expansion of the solution for $\tau \ll q$ with the small τ expansion of the solution for $\tau \gg q$ as

$$\begin{aligned} G_{LL}(\tau) &\approx \frac{1}{2} + \frac{1}{q}\log\frac{2\alpha}{\mathcal{J}} - \frac{\gamma}{q} - \frac{\alpha\tau}{q} \approx A\left(\cosh\frac{\nu\beta}{2} - \nu\tau\sinh\frac{\nu\beta}{2}\right), \\ -iG_{LR}(\tau) &\approx \frac{1}{2} + \frac{1}{q}\log\frac{2\tilde{\alpha}}{\tilde{\mathcal{J}}} - \frac{\tilde{\gamma}}{q} - \frac{\tilde{\alpha}\tau}{q} \approx A\left(\sinh\frac{\nu\beta}{2} - \nu\tau\cosh\frac{\nu\beta}{2}\right), \end{aligned} \tag{4.23}$$

we find the integration constants as

$$\tilde{\alpha} = \alpha, \qquad \tilde{\gamma} = \gamma + s + \sigma, \qquad \alpha = \mathcal{J}\sinh\gamma, \qquad \hat{\mu} = 2\tilde{\alpha}\tanh\tilde{\gamma}. \tag{4.24}$$

Using the relation between the correlation functions and the energy (2.16), we obtain

$$\begin{aligned} \frac{E}{N} &= \frac{1}{2q}\partial_\tau g_{LL}(0) + \frac{1}{2q}\partial_\tau g_{RR}(0) + i\mu\left(1-\frac{2}{q}\right)\frac{i}{2}\left(1+\frac{1}{q}g_{LR}(0)\right) \\ &= -\frac{2\mathcal{J}}{q^2}\cosh\gamma - \frac{\hat{\mu}}{2q} + \frac{\hat{\mu}}{q^2}\left(1+\log\frac{e^s\sinh\gamma}{\cosh\tilde{\gamma}}\right). \end{aligned} \tag{4.25}$$

The effective action $\ell = \frac{1}{N}\log Z$ is then (see appendix A)

$$\ell(\sigma,\gamma) = \frac{\tanh\tilde{\gamma}\log\frac{q}{\sigma}}{q}\left(\frac{q}{2} - 1 + \frac{1}{\tanh\gamma\tanh\tilde{\gamma}} + \log\frac{\sinh\gamma}{\cosh\tilde{\gamma}} + \frac{\sigma}{\tanh\tilde{\gamma}} + s\right) + \frac{\sigma}{q}. \tag{4.26}$$

Now we study the free energy $\frac{F}{N} = -\frac{\ell}{\beta}$ for representative $\tilde{\mathcal{J}}$. This can be worked out in the following way. First, we choose $q, \mathcal{J}, \tilde{\mathcal{J}}, \hat{\mu}$ to a particular set of values. Then, by using the relations $\hat{\mu} = 2\mathcal{J}\sinh\gamma\tanh\tilde{\gamma}$ (4.24) and $\beta = -\frac{1}{2\mathcal{J}\sinh\gamma}\log\frac{\sigma}{q}$ we can compute $\gamma(\sigma)$ and $T(\sigma) = \beta(\sigma)^{-1}$ as functions of σ, with which the data points $(T(\sigma), -\frac{\ell(\sigma,\gamma(\sigma))}{\beta(\sigma)})$ for the free

JHEP04(2023)145

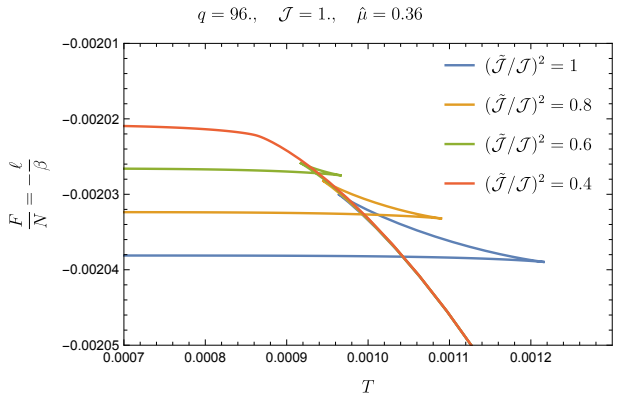

Figure 12. Plot of the free energy as a function of the temperature for representative $\tilde{\mathcal{J}}/\mathcal{J}$.

energy can be generated. The plot of the free energy as a function of T for representative $(\tilde{\mathcal{J}}/\mathcal{J})^2$ is shown in figure 12. In figure 13, we plot the phase diagram for representative $(\tilde{\mathcal{J}}/\mathcal{J})^2$ with $q = 96$. Clearly, we can see that the phase transition exists for small $\hat{\mu}$ and T for sufficiently large $\tilde{\mathcal{J}}$. However, as we decrease $\tilde{\mathcal{J}}$ finally the phase transition disappears for any $\hat{\mu}$ and $\mathcal{J}$ (in the example of $q = 96, \hat{\mu} = 0.36$ and $\mathcal{J} = 1$ in figure 12 the phase transition does not exist for $(\tilde{\mathcal{J}}/\mathcal{J})^2 = 0.4$). In figure 14, we show the phase boundaries $T_{c,2BH}$ and $T_{c,WH}$ for the same $\tilde{\mathcal{J}}$ simultaneously. We see that the power of μ in $T_{c,2BH}$ is not changed much but $T_{c,WH}$ becomes more straight for smaller $\tilde{\mathcal{J}}$.

The phase transition is replaced by crossover at $\mu = \mu_*$ where $T_{c,2BH}$ and $T_{c,WH}$ meet in the phase diagrams. We call this temperature T_*. We plot μ_* and T_* as a function in $\tilde{\mathcal{J}}/\mathcal{J}$ in figure 15. In particular, $\mu_* = 0$ when $\tilde{\mathcal{J}} \approx 0.50\mathcal{J}$ for $q = 96$, where phase transition itself entirely disappears. For smaller $\tilde{\mathcal{J}}$ the phase transition does not exist for all μ and we only see the crossover. In particular, we can confirm the disappearance of the phase transition at finite $\tilde{\mathcal{J}}/\mathcal{J}$ from the large q analysis.

4.3 Absence of phase transitions for small $\tilde{\mathcal{J}}/\mathcal{J}$

Let us regard $(\mathcal{J}, \tilde{\mathcal{J}}, \hat{\mu}, \sigma)$ as fundamental variables instead of $(\mathcal{J}, \tilde{\mathcal{J}}, \hat{\mu}, T)$ and express T as a function of σ (and $\mathcal{J}, \tilde{\mathcal{J}}, \hat{\mu}$) as explained above. When $(\tilde{\mathcal{J}}/\mathcal{J})^2$ is sufficiently large and $\hat{\mu}$ is sufficiently small, $T(\sigma)$ is not a monotonic function of σ, hence a single point in T-μ plane may correspond to several different values of σ. On such a point, different phases corresponding to each value of σ coexist together. On the other hand, when $T(\sigma)$ is monotonic, there are no phase transitions since $\ell(\sigma)$ is a smooth function, and hence the free energy F is a smooth function of the temperature T.

Now we study the monotonicity of $\beta(\sigma)$. The derivative of $\beta(\sigma)$ is

$$\frac{d\beta}{d\sigma} \equiv \frac{d\beta(\gamma(\sigma),\sigma)}{d\sigma} = \frac{q}{\hat{\mu}} \tanh\tilde{\gamma}\left(\frac{\log\frac{q}{\sigma}}{\sinh\tilde{\gamma}\cosh\tilde{\gamma} + \tanh\gamma} - \frac{1}{\sigma}\right). \tag{4.27}$$

Here we used the chain rule $\frac{d\beta}{d\sigma} = \frac{d\gamma}{d\sigma}\frac{\partial\beta}{\partial\gamma} + \frac{\partial\beta}{\partial\sigma}$, together with $\frac{d\gamma(\sigma)}{d\sigma} = -\frac{\tanh\gamma}{\sinh\tilde{\gamma}\cosh\tilde{\gamma}+\tanh\gamma}$ which follows from the relation $\hat{\mu} = 2\mathcal{J}\sinh\gamma\tanh\tilde{\gamma}$ (4.24). Here we take the σ derivative while keeping $\hat{\mu}$. For $\tilde{\mathcal{J}} = \mathcal{J}$, which is the equal coupling in left and right, (4.27) is not

JHEP04(2023)145

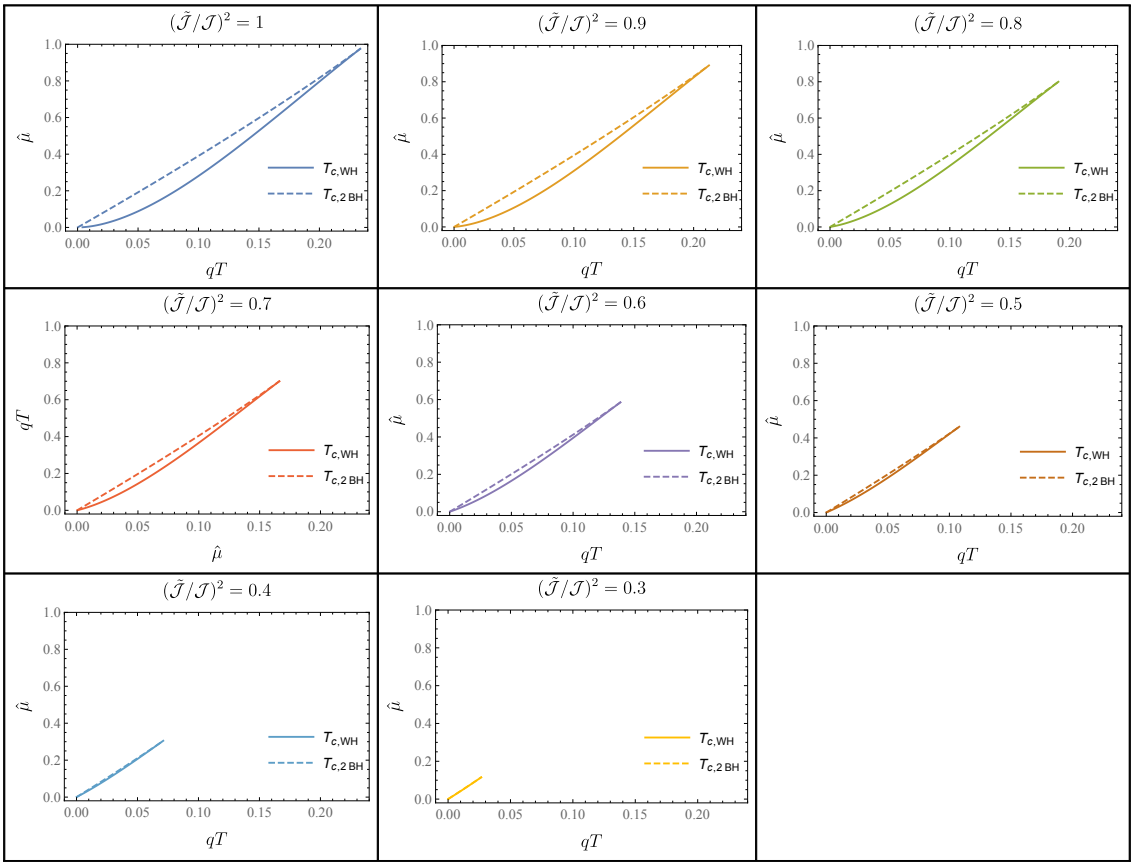

Figure 13. The plots of phase diagrams for representative $\tilde{\mathcal{J}}$.

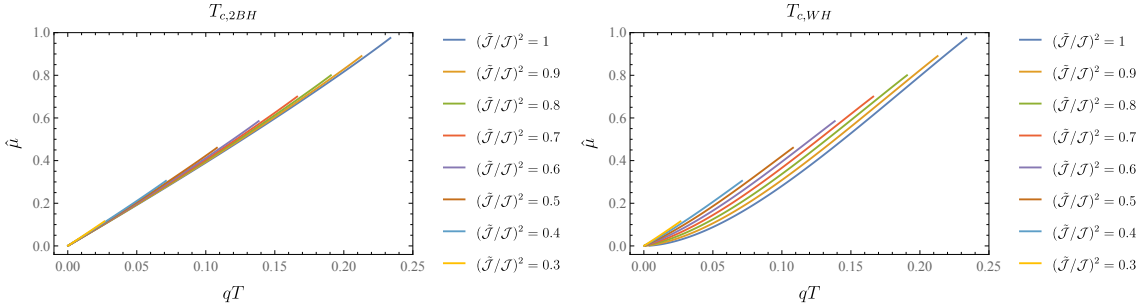

Figure 14. Plots of $T_{c,2BH}$ and $T_{c,WH}$. The parameters are taken to be $\mathcal{J} = 1$, $q = 96$.

monotonic for sufficiently small $\hat{\mu}$ and shows the first-order phase transition. In figure 13, we have observed that as $\tilde{\mathcal{J}}/\mathcal{J}$ is decreased, μ_*, the critical value of μ where the phase transition disappears becomes smaller. When $\tilde{\mathcal{J}}/\mathcal{J}$ crosses some critical value, μ_* finally reaches zero, where the phase transition completely disappears on the (μ, T)-plane. To determine this critical value of $\tilde{\mathcal{J}}/\mathcal{J}$ as a function of q, let us consider the limit $\hat{\mu} \to 0$,

JHEP04(2023)145

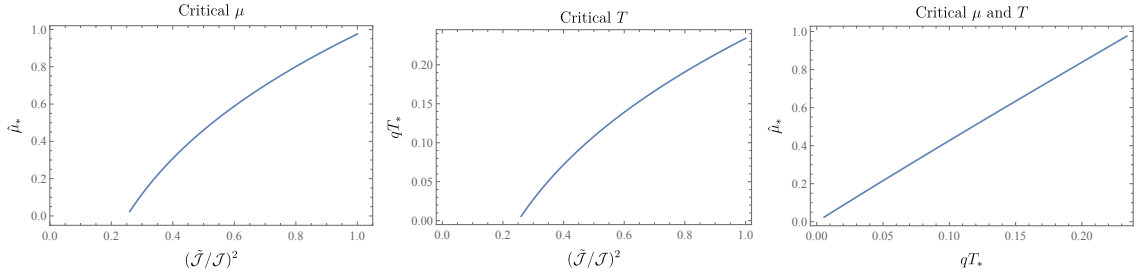

Figure 15. Plots of T_* and μ_*. The parameters are taken to be $\mathcal{J} = 1$, $q = 96$. *Left*: plot of critical μ as a function of $\tilde{\mathcal{J}}/\mathcal{J}$. *Middle*: plot of critical T as a function of $\tilde{\mathcal{J}}/\mathcal{J}$. *Right*: parametric plot of $T_*(\tilde{\mathcal{J}}/\mathcal{J})$ and $\mu_*(\tilde{\mathcal{J}}/\mathcal{J})$.

which gives us

$$\gamma(\sigma) \approx \frac{\hat{\mu}}{2\mathcal{J}\tanh(s+\sigma)}, \quad \frac{d\beta}{d\sigma} \approx \frac{q}{2\hat{\mu}\sigma\cosh^2(s+\sigma)}\left(\frac{2\sigma\log\frac{q}{\sigma}}{1+\frac{\hat{\mu}}{\sinh^2(s+\sigma)}} - \sinh(2s+2\sigma)\right). \tag{4.28}$$

We are interested only in whether $\frac{d\beta}{d\sigma}$ flips its sign or not. Writing $\frac{d\beta}{d\sigma}$ in the following form

$$\frac{d\beta}{d\sigma} = (positive) \times \left(2\sigma\log\frac{q}{\sigma} - \sinh(2s+2\sigma)\right), \tag{4.29}$$

we find that the last factor is negative at $\sigma \to 0, \infty$ and gain its maximum at some finite σ_* where $\frac{d}{d\sigma}(\frac{d\beta}{d\sigma})|_{\sigma_*} = 0$, which is given by

$$2\log\frac{q}{\sigma_*} - 2 - 2\cosh(2s+2\sigma_*) = 0. \tag{4.30}$$

Hence the critical value of $(\tilde{\mathcal{J}}/\mathcal{J})^2$ is determined by the condition $\frac{d\beta}{d\sigma}|_{\sigma_*} = 0$. Solving this condition numerically we obtain figure 16. In particular, when $q = 96$ we obtain $\tilde{\mathcal{J}}/\mathcal{J} = 0.500577$, which is consistent with the critical value we have observed in the previous section.

If we further consider the case $\tilde{\mathcal{J}} \ll \mathcal{J}$, i.e., $s \gg 1$, the condition (4.30) for σ_* reduces to $\log\frac{q}{\sigma_*} \approx \frac{1}{2}e^{2s}$, and the condition $\frac{d\beta}{d\sigma}|_{\sigma_*} = 0$ gives the critical value of $(\tilde{\mathcal{J}}/\mathcal{J})^2$ as

$$\left(\frac{\tilde{\mathcal{J}}}{\mathcal{J}}\right)^2 \approx \frac{1}{2\log(2q)}. \tag{4.31}$$

This result also suggests that the phase transition remains in the limit $q \to \infty$ as far as the $J^{(L)}_{i_1\cdots i_q}$ and $J^{(R)}_{i_1\cdots i_q}$ are correlated even slightly.

The derivative of ℓ is

$$\begin{aligned}\frac{d\ell}{d\sigma} &= \left(\frac{\log\frac{q}{\sigma}}{\sinh\tilde{\gamma}\cosh\tilde{\gamma}+\tanh\gamma} - \frac{1}{\sigma}\right)\frac{1}{\log\frac{q}{\sigma}}\beta\frac{\partial\ell}{\partial\beta} \\ &= \frac{q}{\hat{\mu}\tanh\tilde{\gamma}\log\frac{q}{\sigma}}\frac{d\beta}{d\sigma}\beta\frac{\partial\ell}{\partial\beta}.\end{aligned} \tag{4.32}$$

Since $\frac{\partial\ell}{\partial\beta} = -E/N$ is always positive from the expression (4.25), $\ell(\sigma)$ is also a monotonic function when $\beta(\sigma)$ is monotonic. Therefore, when $\beta(\sigma)$ is monotonic the free energy F is also a monotonic function of the temperature T.

JHEP04(2023)145

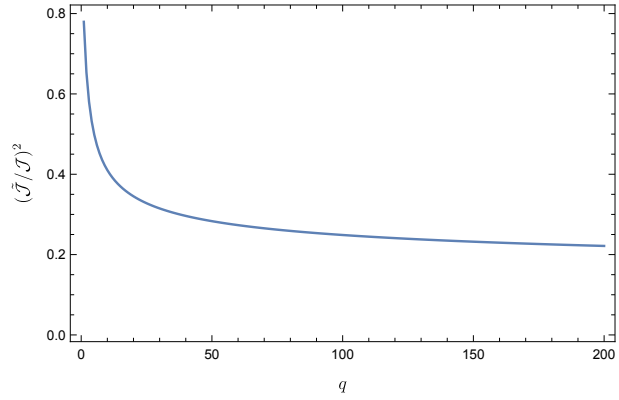

Figure 16. The critical value of $(\tilde{\mathcal{J}}/\mathcal{J})^2$ in the large q approximation where the phase transition becomes a smooth crossover in the entire $(\hat{\mu}, T)$-plane.

4.4 Inverse temperature of order $\beta \sim q$ and beyond

First, we consider the order of $\beta \sim q$. In this regime, G_{LR} is smaller than $1/2$ even for $\tau \ll q$. Therefore we can put $G^q_{LR} = 0$ for $\tau \gg q$ and the effective decay rate ν becomes the naive one $\nu = \mu$. Matching with the solution with $\tau \ll q$ regime we obtain

$$\alpha = \mathcal{J} \sinh \gamma = \frac{\hat{\mu}}{2} \tanh \frac{\beta\mu}{2}. \tag{4.33}$$

The ratio $\tilde{\mathcal{J}}/\mathcal{J}$ does not enter in the correlation function and $\tilde{\mathcal{J}}$ dependence disappears at the order of $\beta \sim q$. Indeed the correlation function and the partition function take the same form both in Maldacena-Qi model [31] and Kourkoulou-Maldacena model [36]. Since the behaviors are exactly the same for any $\tilde{\mathcal{J}}$, we only quote the results from [31, 36] in this paper.

The free energy now becomes

$$-\frac{\beta F}{N} = \log\left(2\cosh\frac{\beta\mu}{2}\right) + \frac{\beta\mu}{q}\tanh\frac{\beta\mu}{2}\left[\log(2\sinh\gamma) + \frac{1}{\tanh\gamma} - \gamma - 1\right]. \tag{4.34}$$

This is independent from the ratio $\tilde{\mathcal{J}}/\mathcal{J}$ and does not depend on the incompleteness of the correlation of the random couplings.

At the order of $\beta \sim \sqrt{q}$, the chaos exponent increases from very small value and finally saturates the chaos bound [31, 36]. The correlation function G_{LR} at this order becomes

$$G_{LR}(\tau) = \frac{i}{2}\mu\left(\frac{\beta}{2} - \tau\right), \tag{4.35}$$

which is of order $1/\sqrt{q}$. The free energy is

$$-\frac{\beta F}{N} = \log 2 + \frac{(\beta\mu)^2}{8} + \frac{2\beta\mathcal{J}}{q^2} + \frac{(\beta\mu)^2}{2q}\log(\beta\mathcal{J}) + \frac{h[q(\beta\mu)^2]}{q^2}. \tag{4.36}$$

where h is a function that we have not determined.

JHEP04(2023)145

At the order of $\beta \sim 1$, we can set $\mu = 0$ to compute g_{LL}, g_{RR} and we recover the decoupled SYK models at large q limit. The free energy is

$$\frac{F}{N} = \frac{2F_{\rm SYK}}{N} - \frac{\beta\mu^2}{8}, \tag{4.37}$$

where $F_{\rm SYK}$ is the free energy of the SYK.

4.4.1 Comments on subleading Lyapunov exponents

At finite q, we have found that there is a subleading Lyapunov exponents in the $\sigma = -1$ sector. In the large q perspective, the problem to find Lyapunov exponents reduces to studying the bound states of a Schrödinger equation, and we would be able to understand the subleading Lyapunov exponents using that language as follows. At $\mu = 0$ we have two copies of the SYK and the Lyapunov exponents are degenerate. After introducing μ, two degeneracies are resolved and we will get two different exponents, which leads to the subleading Lyapunov exponents.

However, at the leading order of $1/q$ expansion, the degeneracy is not resolved because σ dependent term is actually of order $1/q$ at large q limit. By taking the large q limit of (3.16), we obtain

$$\begin{aligned} &M_{1,LLLL}(t) \propto (G^R_{LL})^2 = O(1), \qquad M_{1,LLLR}(t) \propto G^R_{LL}G^R_{LR} = O(1/\sqrt{q}), \\ &M_{1,LRLR}(t) \propto (G^R_{LR})^2 = O(1/q), \qquad M_{2,LL}(t) = -2\mathcal{J}^2 e^{g_{LL}(\beta/2+it)}, \qquad M_{2,LR}(t) = 0, \end{aligned} \tag{4.38}$$

where we have used the fact that G_{LR} is of order $1/\sqrt{q}$. Therefore the only surviving terms at the large q are $M_{1,LLLL}(t)$ and $M_{2,LL}(t)$ and we find that σ dependent terms drop at the leading order in the $1/q$ expansion. This means that what we get is the degenerate Lyapunov exponents at any temperature at large q. We hope to investigate the subleading corrections in the $1/q$ expansion to see the resolution of the degeneracy in future works.

5 Structure of ground state for imperfectly correlated disorders

In this section, we investigate the structure of the ground state of the coupled model (2.1). Let us consider the following state $|I(\beta)\rangle$

$$|I(\beta)\rangle = \frac{1}{\mathcal{N}} e^{-\frac{\beta}{4}(H^{(L)}_{\rm SYK}+H^{(R)}_{\rm SYK})}|I\rangle, \tag{5.1}$$

where $|I\rangle$ is the ground state of $H_{\rm int} = i\sum_{i=1}^N \psi^L_i \psi^R_i$ and $\mathcal{N} = \sqrt{\langle I|e^{-\frac{\beta}{2}(H^{(L)}_{\rm SYK}+H^{(R)}_{\rm SYK})}|I\rangle}$ is the normalization factor. When the correlation of $J^{(L)}_{i_1\cdots i_q}$ and $J^{(R)}_{i_1\cdots i_q}$ is perfect, this state is the thermofield double state. Therefore the state $|I(\beta)\rangle$ is a generalization of the thermofield double state. In the limit $\mu \to \infty$, the ground state of H approaches $|I(\beta)\rangle$ with $\beta = 0$. Also in the limit $\beta \to \infty$, $|I(\beta)\rangle$ is approximated with the ground state of $H^{(L)}_{\rm SYK} + H^{(R)}_{\rm SYK}$. If we assume that the ground state of $H^{(L)}_{\rm SYK} + H^{(R)}_{\rm SYK}$ is non-degenerate, it coincides with the ground state of the coupled model in the limit $\mu \to 0$. Therefore $|I(\beta)\rangle$

JHEP04(2023)145

should be a good one-parameter ansatz to approximate the ground state of the two-coupled system (2.1) at least in the limit $\mu \to \infty$ and $\mu \to 0$. When the two random couplings are perfectly correlated, $|I(\beta)\rangle$ was found to be a good approximation of the ground state also for finite μ [31, 34, 35]. In this section, we provide some pieces of evidence that $|I(\beta)\rangle$ approximates the ground state for finite μ well even when the correlation between $J^{(L)}_{i_1\cdots i_q}$ and $J^{(R)}_{i_1\cdots i_q}$ is imperfect.

5.1 Variational approximation in large q limit

To understand the ground state for $\langle J^{(L)}_{i_1\cdots i_q} J^{(R)}_{i_1\cdots i_q}\rangle < \langle (J^{(L)}_{i_1\cdots i_q})^2\rangle$, here we study the variational approximation by the generalized thermofield double state

$$|I(\beta)\rangle = \frac{1}{\sqrt{Z_{LR}}} e^{-\frac{\beta}{4}H_L} e^{-\frac{\beta}{4}H_R} |I\rangle\,. \tag{5.2}$$

Here $|I\rangle$ is the maximally entangled state defined by

$$\psi^i_L |I\rangle = -i\psi^i_R |I\rangle\,. \tag{5.3}$$

This is the ground state of the coupling Hamiltonian $H_{\rm int} = -i\mu \sum_{i=1}^N \psi^i_L \psi^i_R$. Z_{LR} is the normalization factor defined by

$$Z_{LR} = \langle I|\, e^{-\frac{\beta}{2}H_L} e^{-\frac{\beta}{2}H_R} |I\rangle = {\rm Tr}(e^{-\frac{\beta}{2}H_{\rm SYK}(J^{(L)}_{i_1\cdots i_q})} e^{-\frac{\beta}{2}H_{\rm SYK}(J^{(R)}_{i_1\cdots i_q})}). \tag{5.4}$$

Here $H_{\rm SYK}(J_{i_1\cdots i_q})$ is the SYK Hamiltonian with the random coupling $J_{i_1\cdots i_q}$ acting on a single-side Hilbert space. In Maldacena-Qi model, choosing an appropriate β, $|I(\beta)\rangle$ is a very good approximation for the exact ground state in the sense that the leading term of the overlap between them becomes 1 in the small μ limit or in the large q limit. In Kourkoulou-Maldacena model, this state is still a good approximation in the sense that the leading overlap is 1 at large q. Therefore, we expect that the state $|I(\beta)\rangle$ is a good approximation for the exact ground state even when the correlation of $J^{(L)}_{i_1\cdots i_q}$ and $J^{(R)}_{i_1\cdots i_q}$ is imperfect.

We study the variational approximation by $|I(\beta)\rangle$ at large q. To do that, we minimize the trial energy

$$E_{\rm trial}(\beta) = \langle I(\beta)|H_L + H_R + H_{\rm int}|I(\beta)\rangle\,. \tag{5.5}$$

In terms of the Euclidean correlation functions on the thermal circle with interfaces which are schematically depicted in figure 17, the trial energy is

$$E_{\rm trial}(\beta) = \frac{1}{q}\partial_\tau G_{LL}(\tau,0)\Big|_{\tau\to 0_+} + \frac{1}{q}\partial_\tau G_{LR}(\tau,0)\Big|_{\tau\to 0_+} + i\mu G_{LR}(0,0). \tag{5.6}$$

JHEP04(2023)145

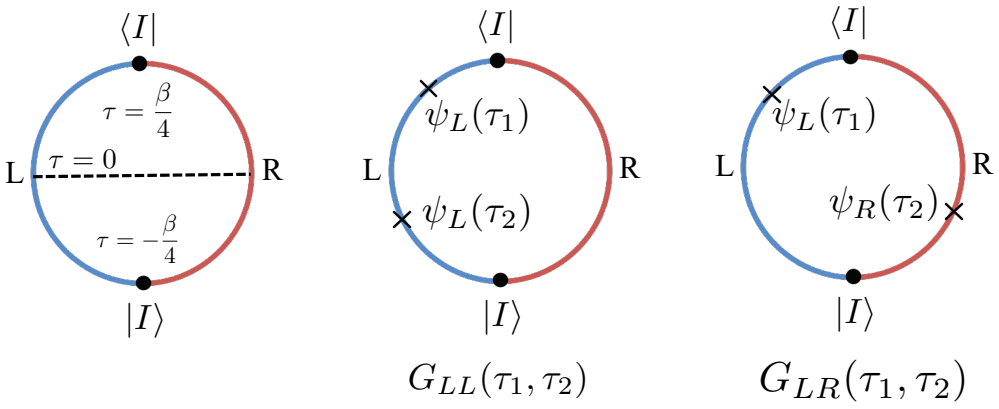

Figure 17. The schematic pictures of the correlation functions. *Left*: the path integral representation for the partition function Z_{LR}. *Middle*: the correlation function G_{LL}. *Right*: the correlation function G_{LR}.

In the large q limit, the correlation function becomes $G_{\alpha\beta}(\tau_1,\tau_2) = G_{0,\alpha\beta}\Big(1+\frac{1}{q}g_{\alpha\beta}(\tau_1,\tau_2)\Big)$ with [50, 51]

$$e^{g_{LL}(\tau_1,\tau_2)} = e^{g_{RR}(\tau_1,\tau_2)} = \left(\frac{\check{\alpha}}{\mathcal{J}\sin(\check{\alpha}|\tau_1-\tau_2|+\check{\gamma})}\right)^2, \quad \text{for} \quad -\frac{\beta}{4} < \tau_1,\tau_2 < \frac{\beta}{4},$$
$$e^{g_{LR}(\tau_1,\tau_2)} = \left(\frac{\check{\alpha}^2/\mathcal{J}^2}{-\lambda^2\sin\Big(\check{\alpha}\Big(\tau_1+\frac{\beta}{4}\Big)\Big)\sin\Big(\check{\alpha}\Big(\tau_2-\frac{\beta}{4}\Big)\Big)+\sin\Big(\check{\alpha}\Big(\frac{\beta}{4}-\tau_1\Big)+\check{\gamma}\Big)\sin\Big(\check{\alpha}\Big(\frac{\beta}{4}-\tau_2\Big)+\check{\gamma}\Big)}\right)^2,$$
$$\text{for} \quad -\frac{\beta}{4} < \tau_1,\tau_2 < \frac{\beta}{4}. \tag{5.7}$$

Here we have introduced a parameter $\lambda = \tilde{\mathcal{J}}/\mathcal{J}$. The parameters $\check{\alpha}$ and $\check{\gamma}$ satisfy

$$\check{\alpha} = \mathcal{J}\sin\check{\gamma}, \qquad \sin\left(\frac{\check{\alpha}\beta}{2}+2\check{\gamma}\right) = \lambda^2\sin\left(\frac{\check{\alpha}\beta}{2}\right). \tag{5.8}$$

Then, $E_{\text{trial}}(\beta)$ becomes

$$E_{\text{trial}}(\beta) = -\frac{2\mathcal{J}}{q^2}\cos\check{\gamma} - \frac{\hat{\mu}}{2q} - \frac{\hat{\mu}}{q^2}\log\left[\frac{\sin^2\check{\gamma}}{(1-\lambda^2)+\sqrt{(1-\lambda^2)^2+4\lambda^2\sin^2\check{\gamma}}}\right]. \tag{5.9}$$

Here we have used the relation

$$\frac{1}{q}\partial_\tau G_{LL}(\tau,0)\Big|_{\tau\to 0_+} = -\frac{\mathcal{J}}{q^2}\cos\check{\gamma},$$
$$e^{g_{LR}(0,0)} = \left(\frac{\check{\alpha}^2/\mathcal{J}^2}{-\lambda^2\sin^2\frac{\check{\alpha}\beta}{4}+\sin^2(\frac{\check{\alpha}\beta}{4}+\check{\gamma})}\right)^2 = \left(\frac{2\sin^2\check{\gamma}}{(1-\lambda^2)+\sqrt{(1-\lambda^2)^2+4\lambda^2\sin^2\check{\gamma}}}\right)^2. \tag{5.10}$$

JHEP04(2023)145

Because of the chain rule, we can instead take the derivative w.r.t. $\check{\gamma}$ to minimize the trial energy:

$$q^2\frac{\partial E_{\text{trial}}}{\partial\check{\gamma}} = 2\mathcal{J}\sin\check{\gamma} - \frac{\hat{\mu}}{\tan\check{\gamma}}\frac{(1-\lambda^2)+\sqrt{(1-\lambda^2)^2+4\lambda^2\sin^2\check{\gamma}}}{\sqrt{(1-\lambda^2)^2+4\lambda^2\sin^2\check{\gamma}}} = 0. \tag{5.11}$$

This equation is solved as

$$\cos\check{\gamma} = \cosh\gamma - \sinh\gamma\tanh\tilde{\gamma}, \tag{5.12}$$

where γ is the solution of the equation (4.8). This determines the variational parameter β as a function of μ.

We find that the SYK energy and the expectation value of the interaction Hamiltonian completely agree:

$$\begin{aligned}\langle G(\mu)|H_L+H_R|G(\mu)\rangle &= \langle I(\beta(\mu))|H_L+H_R|I(\beta(\mu))\rangle = -\frac{2\mathcal{J}}{q^2}\cos\check{\gamma},\\ \langle G(\mu)|\psi_L\psi_R|G(\mu)\rangle &= \langle I(\beta(\mu))|\psi_L\psi_R|I(\beta(\mu))\rangle = \frac{i}{2}\left[1+\frac{1}{q}\log\left(\frac{e^s\sinh\gamma}{\cosh\tilde{\gamma}}\right)^2\right].\end{aligned} \tag{5.13}$$

Therefore, the variational energy actually is equal to the true energy (4.25)

$$E_{\text{trial}}(\beta(\mu)) = E_g. \tag{5.14}$$

This means that the $|I(\beta(\mu))\rangle = |G(\mu)\rangle$ in the large q limit.

5.2 Overlap between ground state and $|I(\beta)\rangle$ for finite q

In the previous section we have found that $|I(\beta)\rangle$ (5.1), with $\beta(\mu)$ chosen appropriately, approximates the energy of the ground state well when both q and N are large. This is strong evidence that $|I(\beta)\rangle$ approximates well the true ground state $|gs\rangle$ of the two-coupled Hamiltonian (2.1). In this section, we study the validity of this approximation for finite q by comparing the two states directly for finite N.

Note that there are several subtleties. First, since the full Hamiltonian as well as $i\sum_{i=1}^N\psi_i^L\psi_i^R$ commute with the fermion number parity Γ_c (B.4), both $|I(\beta)\rangle$ and the ground state of H are eigenstates of Γ_c. When μ is not sufficiently large, the parity of the ground state of H depends on the realization of $J^{(a)}_{i_1\cdots i_q}$ and hence is not always the same as the parity of $|I(\beta)\rangle$. Hence to make the comparison reasonable we should compare $|I(\beta)\rangle$ with $|gs,(-1)^{\frac{N(N-1)}{2}}\rangle$, the eigenstate of H with the lowest energy in the same parity sector as $|I(\beta)\rangle$, $\Gamma_c=(-1)^{\frac{N(N-1)}{2}}$, rather than the true ground state of H.

Second, although $|I(\beta)\rangle$ approximates well the ground state at $\mu\approx 0$ when the ground state of $H^{(L)}_{\text{SYK}}+H^{(R)}_{\text{SYK}}$ is non-degenerate, the spectrum of single SYK Hamiltonian has the following degeneracy depending on the value of q and N mod 8 [52]:

q, N	degeneracy of single SYK spectrum
$q=0$ mod 4, $\quad N=2,6$ mod 8	2 (between different parity sectors)
$q=0$ mod 4, $\quad N=4$ mod 8	2 (in each parity sector)
$q=0$ mod 4, $\quad N=0$ mod 8	non-degenerate
$q=2$ mod 4	non-degenerate

, (5.15)

JHEP04(2023)145

which implies that the ground state of $H^{(L)}_{\rm SYK}+H^{(R)}_{\rm SYK}$ is also degenerate in the cases of the first two rows. On the other hand, $|I\rangle$ contains only a certain linear combination of them (which can be identified explicitly for $J^{(L)}_{i_1\cdots i_q}=J^{(R)}_{i_1\cdots i_q}$ case, as summarized in appendix B). Note that this degeneracy cannot be removed completely by the total fermion number parity Γ_c. When μ is small but non-zero, the degeneracy is removed and the true ground state is approximately a certain linear combination of the degenerate ground states at $\mu=0$. This linear combination varies depending on the realization of $J^{(a)}_{i_1\cdots i_q}$ and is not necessarily the same as the linear combination contained in $|I\rangle$.

To avoid these subtleties, here we choose $q=6$ where the ground state in $\Gamma_c=(-1)^{\frac{N(N-1)}{2}}$ sector at $\mu=0$ is non-degenerate for any N, and consider the overlap between $|I(\beta)\rangle$ and $|gs,(-1)^{\frac{N(N-1)}{2}}\rangle$, maximized with respect to β. As a result, we obtain figure 18. The results suggest that $|I(\beta)\rangle$ is indeed a good approximation to $|gs,(-1)^{\frac{N(N-1)}{2}}\rangle$ also for finite μ.

6 Discussion and future works

In this paper, we have studied the thermodynamic and chaotic properties of the two-coupled SYK model where the two random couplings are not completely the same. As a result, we have found that the phase transition temperature becomes smaller as the correlation of the random couplings is reduced. This is consistent with the intuition that the correlation between the random couplings makes it easier for the wormhole to form between the two sides.

Then, we have studied the properties of the ground state of the coupled SYK model with an imperfect correlation of the random couplings. As we change the correlation, the behavior of the energy gap also changes. When $\tilde{\mathcal{J}}/\mathcal{J}$ is close to 1, the SYK interaction still helps to make the gap larger than the naive one $E_{\rm gap}\sim\mu$. However, as we decrease μ, finally the effect of imperfect correlation wins, and the energy gap becomes smaller than the naive one, which we expect when we have no correlation between $J^{(L)}_{i_1\cdots i_q}$ and $J^{(R)}_{i_1\cdots i_q}$. For $\tilde{\mathcal{J}}$ where the thermal phase transition disappears, the energy gap is close to that without $\langle J^{(L)}_{i_1\cdots i_q}J^{(R)}_{i_1\cdots i_q}\rangle$ correlation as far as we have checked.

We have also found that the transmission amplitude between the two sides in the wormhole phase for fixed temperature T and the direct LR coupling μ becomes smaller as the correlation of the random couplings is reduced. On the other hand, as the correlation is reduced the largest chaos exponent becomes larger. Assuming that the largest chaos exponent is associated with the information spreading within each side rather than between the two sides, this behavior of the chaos exponent is also consistent with the same intuition. Interestingly, we have also found that the phase transition completely disappears when the correlation between the random couplings is smaller than some non-zero finite value which is around $\langle J^{(L)}_{i_1\cdots i_q}J^{(R)}_{i_1\cdots i_q}\rangle\approx 0.3\langle (J^{(L)}_{i_1\cdots i_q})^2\rangle$ for $q=4$ and $\langle J^{(L)}_{i_1\cdots i_q}J^{(R)}_{i_1\cdots i_q}\rangle\sim(\log q)^{-1}\langle (J^{(L)}_{i_1\cdots i_q})^2\rangle$ for large q.

Finally, to understand the properties of the ground state, we have studied how it is close to the generalized thermofield double state (5.1). This generalized theromfield double state has a jump of couplings in Euclidean time and is studied in the context of

JHEP04(2023)145

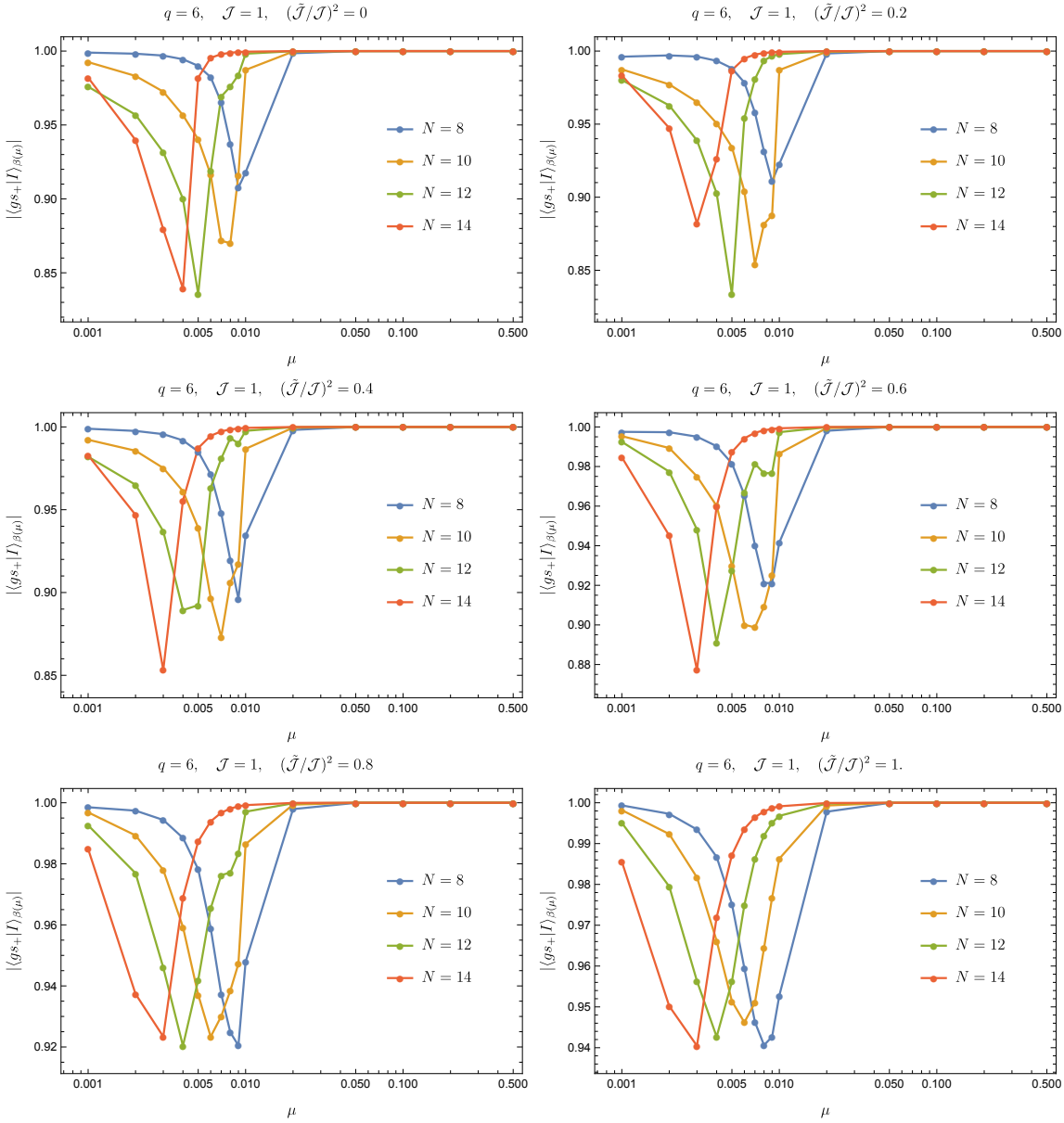

Figure 18. The overlap $|\langle I_\beta|gs, (-1)^{\frac{N(N-1)}{2}}\rangle|$ maximized with respect to β.

black holes [26–28, 30]. It turns out that the ground state coincides with the generalized thermofield double state at large q. In this sense, the coupled Hamiltonian prepares an "SYK Janus black hole" as its ground state. In the case of SYK Janus black holes, we have an expanded interior. Intuitively, this expanded interior makes the length between the two mouths of the wormholes longer and it takes more time to traverse the wormhole. This is an intuitive explanation for why E_{gap}, which is roughly the time to traverse the wormhole, becomes larger for smaller $\tilde{\mathcal{J}}/\mathcal{J}$.

In section 3.3.2 we have found that the ladder kernel for the four-point functions can be block-diagonalized into two sectors labeled by $\sigma = \pm 1$, and have observed that the

JHEP04(2023)145

chaos exponent in the $\sigma = -1$ sector vanishes at some temperature $T = T_{c,\mathrm{Ly}}(\mu, \tilde{\mathcal{J}}/\mathcal{J})$ which is larger than $T_{c,\mathrm{WH}}$ (the vanishing chaos exponent was also observed in [37] for $J^{(L)}_{i_1\cdots i_q} = J^{(R)}_{i_1\cdots i_q}$). It would be interesting to investigate the physical interpretation of this phenomenon. For this purpose, it would be important to reproduce the same phenomenon analytically in the large q limit. As commented in section 4.4.1 this requires the analysis of the sub-leading correction in $1/q$.

In this paper, we have studied the effect of the correlation between $J^{(L)}_{i_1\cdots i_q}$ and $J^{(R)}_{i_1\cdots i_q}$ in the two-coupled model without modifying the probability distributions of each $J^{(a)}_{i_1\cdots i_q}$ themselves. One may also consider different modifications of the distribution of the random couplings such as an imbalanced rescaling $J^{(R)}_{i_1\cdots i_q} = cJ^{(L)}_{i_1\cdots i_q}$ with $c \neq 1$ [53] or the sparse couplings [54–56] instead of full $J^{(a)}_{i_1\cdots i_q}$. It would also be interesting to study how the traversability and other properties of these models change as the correlation between the random couplings on two sides is varied.

One may also adopt different kinds of LR interactions instead of the one $i\sum_i \psi^L_i \psi^R_i$ we have used. For example, the LR interaction can also be turned on by considering $H = f(H^{(L)}_{\mathrm{SYK}} + H^{(R)}_{\mathrm{SYK}})$ with any non-linear function f. Such a transformation of the Hamiltonian naturally arises in the context of $T\bar{T}$ deformation [57–63], whose quench protocol was studied in [64]. It would be interesting to investigate the properties of such models further.

Acknowledgments

We thank Kanato Goto, Cheng Peng, Dario Rosa and Yingyu Yang for valuable discussions and useful comments. The numerical analyses in this paper were performed on sushiki server in Yukawa Institute Compute Facility and on Ulysses cluster v2 in SISSA. T. Numasawa is supported by MEXT KAKENHI Grant-in-Aid for Transformative Research Areas A "Extreme Universe" Grant Number 22H05248.

A A derivation of the large q partition function

The solution for $\tau \ll q$ is

$$\begin{aligned} e^{g_{LL}(\tau)} &= \frac{\alpha^2}{\mathcal{J}^2 \sinh^2(\alpha|\tau| + \gamma)}, \\ e^{g_{LR}(\tau)} &= \frac{\tilde{\alpha}^2}{\tilde{\mathcal{J}}^2 \cosh^2(\tilde{\alpha}|\tau| + \tilde{\gamma})}, \end{aligned} \tag{A.1}$$

and for $\tau \gg q$

$$\begin{aligned} G_{LL}(\tau) &= A \cosh\left[\nu\left(\frac{\beta}{2} - \tau\right)\right], \\ G_{LR}(\tau) &= iA \sinh\left[\nu\left(\frac{\beta}{2} - \tau\right)\right], \end{aligned} \tag{A.2}$$

JHEP04(2023)145

where

$$\nu = i\int_{-\infty}^{\infty}\Sigma_{LR}(\tau)d\tau = \frac{2\tilde{\alpha}}{q} = \frac{\hat{\mu}}{q\tanh\tilde{\gamma}}. \tag{A.3}$$

In the matching region, G_{LL} and G_{LR} are expanded as

$$\begin{aligned} G_{LL} &\sim \frac{1}{2} - \frac{1}{q}\left(\log\frac{\mathcal{J}}{\alpha} + \gamma + \alpha\tau\right) \sim A\left[\cosh\frac{\nu\beta}{2} - \tau\nu\sinh\frac{\nu\beta}{2}\right] \\ -iG_{LR} &\sim \frac{1}{2} - \frac{1}{q}\left(\log\frac{\tilde{\mathcal{J}}}{\tilde{\alpha}} + \tilde{\gamma} + \tilde{\alpha}\tau\right) \sim A\left[\sinh\frac{\nu\beta}{2} - \tau\nu\cosh\frac{\nu\beta}{2}\right]. \end{aligned} \tag{A.4}$$

This determines the parameters to be

$$\alpha = \tilde{\alpha}, \qquad \tilde{\gamma} = \gamma + \sigma + s. \tag{A.5}$$

Here we have defined σ by

$$\sigma = qe^{-\beta\nu}, \tag{A.6}$$

which is of order $O(1)$. The boundary conditions at $\tau = 0$ give

$$\alpha = \mathcal{J}\sinh\gamma, \qquad \hat{\mu} = 2\tilde{\alpha}\tanh\tilde{\gamma}. \tag{A.7}$$

The conditions (A.5), (A.6) and (A.7) determine the relation between the physical parameters $\hat{\mu}, \mathcal{J}, \tilde{\mathcal{J}}, \beta$ and σ, γ, s. The energy is

$$\begin{aligned} \frac{E}{N} = -\frac{1}{N}\partial_\beta\log Z &= \frac{1}{2q}\partial_\tau g_{LL}(0) + \frac{1}{2q}\partial_\tau g_{RR}(0) + i\mu\left(1-\frac{2}{q}\right)\frac{i}{2}\left(1+\frac{1}{q}g_{LR}(0)\right) \\ &= -\frac{2\mathcal{J}}{q^2}\cosh\gamma - \frac{\hat{\mu}}{2q} + \frac{\hat{\mu}}{q^2}\left(1+\log\frac{e^s\sinh\gamma}{\cosh\tilde{\gamma}}\right). \end{aligned} \tag{A.8}$$

In the following we choose the fundamental variables as either $(\hat{\mu}, \mathcal{J}, s, \beta)$ or $(\sigma, \gamma, s, \beta)$ interchangeably. Using the effective action we can write[6]

$$\begin{aligned} \mathcal{J}\frac{\partial\ell}{\partial\mathcal{J}}\bigg|_{\hat{\mu},s,\beta} &= \beta\int_0^\infty(\mathcal{J}^2e^{g_{LL}} + \tilde{\mathcal{J}}^2e^{g_{LR}})d\tau = \frac{\beta\hat{\mu}}{q^2}\left[\frac{1}{\tanh\gamma\tanh\tilde{\gamma}} - 1\right], \\ \mu\frac{\partial\ell}{\partial\hat{\mu}}\bigg|_{\mathcal{J},s,\beta} &= -i\beta\mu G_{LR}(0) = \frac{\beta\hat{\mu}}{q^2}\left[\frac{q}{2} + \log\left(\frac{\sinh\gamma}{\cosh\tilde{\gamma}}\right) + s\right]. \end{aligned} \tag{A.9}$$

By the change of variables, the partial derivatives are given by

$$\begin{aligned} &\frac{1}{\hat{\mu}}\frac{\partial\hat{\mu}}{\partial\gamma}\bigg|_{\sigma,s,\beta} - \frac{1}{\mathcal{J}}\frac{\partial\mathcal{J}}{\partial\gamma}\bigg|_{\sigma,s,\beta} = \frac{1}{\tanh\gamma} + \frac{1}{\sinh\tilde{\gamma}\cosh\tilde{\gamma}}, \qquad \frac{1}{\beta\hat{\mu}}\frac{\partial(\beta\hat{\mu})}{\partial\gamma}\bigg|_{\sigma,s,\beta} = \frac{1}{\sinh\tilde{\gamma}\cosh\tilde{\gamma}}, \\ &\frac{1}{\hat{\mu}}\frac{\partial\hat{\mu}}{\partial\sigma}\bigg|_{\gamma,s,\beta} - \frac{1}{\mathcal{J}}\frac{\partial\mathcal{J}}{\partial\sigma}\bigg|_{\gamma,s,\beta} = \frac{1}{\sinh\tilde{\gamma}\cosh\tilde{\gamma}}, \qquad \frac{1}{\beta\hat{\mu}}\frac{\partial(\beta\hat{\mu})}{\partial\sigma}\bigg|_{\gamma,s,\beta} = \frac{1}{\sinh\tilde{\gamma}\cosh\tilde{\gamma}} - \frac{1}{\sigma\log\frac{q}{\sigma}}. \end{aligned} \tag{A.10}$$

[6]Here we take the $\mathcal{J}$ derivative with fixed s and $\partial_\mathcal{J}$ also acts on $\tilde{\mathcal{J}}$ terms.

JHEP04(2023)145

Then, the derivative of ℓ in γ, σ is determined through

$$\begin{aligned}
\left.\frac{\partial \ell}{\partial \gamma}\right|_{\sigma,s,\beta} &= \left.\frac{1}{\beta\hat{\mu}}\frac{\partial(\beta\hat{\mu})}{\partial\gamma}\right|_{\sigma,s,\beta} \beta \left.\frac{\partial \ell}{\partial \beta}\right|_{\hat{\mu},\mathcal{J},s} - \left(\left.\frac{1}{\hat{\mu}}\frac{\partial\hat{\mu}}{\partial\gamma}\right|_{\sigma,s,\beta} - \left.\frac{1}{\mathcal{J}}\frac{\partial\mathcal{J}}{\partial\gamma}\right|_{\sigma,s,\beta}\right)\mathcal{J}\left.\frac{\partial\ell}{\partial\mathcal{J}}\right|_{\hat{\mu},s,\beta}, \\
\left.\frac{\partial \ell}{\partial \sigma}\right|_{\gamma,s,\beta} &= \left.\frac{1}{\beta\hat{\mu}}\frac{\partial(\beta\hat{\mu})}{\partial\sigma}\right|_{\gamma,s,\beta} \beta \left.\frac{\partial \ell}{\partial \beta}\right|_{\hat{\mu},\mathcal{J},s} - \left(\left.\frac{1}{\hat{\mu}}\frac{\partial\hat{\mu}}{\partial\sigma}\right|_{\gamma,\beta,s} - \left.\frac{1}{\mathcal{J}}\frac{\partial\mathcal{J}}{\partial\sigma}\right|_{\gamma,\beta,s}\right)\mathcal{J}\left.\frac{\partial\ell}{\partial\mathcal{J}}\right|_{\hat{\mu},s,\beta}.
\end{aligned} \tag{A.11}$$

Here we have used the relation $(\mu\partial_\mu + \mathcal{J}\partial_\mathcal{J} - \beta\partial_\beta)\ell = 0$ since ℓ is a function of dimensionless parameters $\ell(\beta\hat{\mu}, \mathcal{J}\beta, s)$. Integrating (A.11), we obtain

$$\ell(\sigma,\gamma) = \frac{\tanh\tilde{\gamma}\log\frac{q}{\sigma}}{q}\left(\frac{q}{2} - 1 + \frac{1}{\tanh\gamma\tanh\tilde{\gamma}} + \log\frac{\sinh\gamma}{\cosh\tilde{\gamma}} + s + \frac{\sigma}{\tanh\tilde{\gamma}}\right) + \frac{\sigma}{q}, \tag{A.12}$$

which is the result in (4.26). Interestingly, the effect of the incomplete correlation $\mathcal{J} \neq \tilde{\mathcal{J}}$ is included only in $\tilde{\gamma}$ and the partition function takes the same form with the completely correlated random couplings $\mathcal{J} = \tilde{\mathcal{J}}$.

B Relation between ground state of H_{int} and eigenstates of $H^{(a)}_{\text{SYK}}$

In this section we display the explicit relation between $|I\rangle$, the ground state of H_{int} (2.2), and the eigenstates of $H^{(L)}_{\text{SYK}} + H^{(R)}_{\text{SYK}}$ for $J^{(L)}_{i_1\cdots i_q} = J^{(R)}_{i_1\cdots i_q}$. For $q = 4$ the results are also written in [34].

B.1 Gamma matrices and charge conjugation matrix

Let us first fix the convention for the gamma matrices, and also introduce the charge conjugation operator C for single side, which plays a crucial role in fixing the ambiguities of the overall phases of the eigenstates of $H^{(L)}_{\text{SYK}} + H^{(R)}_{\text{SYK}}$.

We choose the representation of the single-side gamma matrices γ_i and single-side fermion number parity matrix γ_c as

$$\begin{aligned}
\gamma_1 &= X\otimes 1\otimes 1\otimes 1\otimes\cdots\otimes 1\otimes 1, \\
\gamma_2 &= Y\otimes 1\otimes 1\otimes 1\otimes\cdots\otimes 1\otimes 1, \\
\gamma_3 &= Z\otimes X\otimes 1\otimes 1\otimes\cdots\otimes 1\otimes 1, \\
\gamma_4 &= Z\otimes Y\otimes 1\otimes 1\otimes\cdots\otimes 1\otimes 1, \\
\gamma_5 &= Z\otimes Z\otimes X\otimes 1\otimes\cdots\otimes 1\otimes 1, \\
&\vdots \\
\gamma_N &= Z\otimes Z\otimes Z\otimes Z\otimes\cdots\otimes Z\otimes Y, \\
\gamma_c &= (-i)^{\frac{N}{2}}\gamma_1\gamma_2\cdots\gamma_N = Z^{\otimes\frac{N}{2}},
\end{aligned} \tag{B.1}$$

where

$$X = \begin{pmatrix} 0 & 1 \\ 1 & 0 \end{pmatrix}, \quad Y = \begin{pmatrix} 0 & -i \\ i & 0 \end{pmatrix}, \quad Z = \begin{pmatrix} 1 & 0 \\ 0 & -1 \end{pmatrix}. \tag{B.2}$$

JHEP04(2023)145

With these γ_i and γ_c, we define the gamma matrices for the two-coupled system $\Gamma_i^{(a)} = \sqrt{2}\psi_i^{(a)}$ $(a = L, R)$ as

$$\Gamma_i^{(L)} = \gamma_i \otimes 1, \quad \Gamma_i^{(R)} = \gamma_c \otimes \gamma_i, \tag{B.3}$$

and define the fermion number parity matrix Γ_c for the two-coupled system as[7]

$$\Gamma_c = (-i)^N \Gamma_1^{(L)} \Gamma_2^{(L)} \cdots \Gamma_N^{(L)} \Gamma_1^{(R)} \Gamma_2^{(R)} \cdots \Gamma_N^{(R)} = \gamma_c \otimes \gamma_c. \tag{B.4}$$

Since $|I\rangle$, the ground state of H_{int} (2.2), satisfies $i\Gamma_i^{(L)}\Gamma_i^{(R)}|I\rangle = -|I\rangle$ for all $i = 1, 2, \cdots, N$, we find that the fermion number parity of $|I\rangle$ is $\Gamma_c = (-1)^{\frac{N(N-1)}{2}}$.

The charge conjugation operator C of single side can be defined as

$$C = \gamma_2 \gamma_4 \cdots \gamma_N K, \tag{B.5}$$

where K is the complex conjugation in the basis which define the matrix element of X, Y, Z as (B.2). Note that $CK = \gamma_2\gamma_4 \cdots \gamma_N$ is a unitary operator but C is not a unitary operator. Let us list several important properties of C:

$$C\gamma_i = (-1)^{\frac{N}{2}} \gamma_i C, \quad C\gamma_c = (-1)^{\frac{N}{2}} \gamma_c C, \quad C^2 = \begin{cases} 1 & (N = 0, 6 \bmod 8) \\ -1 & (N = 2, 4 \bmod 8) \end{cases}, \tag{B.6}$$

$$\langle \phi | \gamma_i | \psi \rangle = (-1)^{\frac{N}{2}} (C|\psi\rangle)^\dagger \gamma_i C |\phi\rangle, \tag{B.7}$$

which we use in the rest of this section.

B.2 $q = 0$ mod 4

For $q = 0$ mod 4, $H_{\text{SYK}}^{(L)}$ and $H_{\text{SYK}}^{(R)}$ with $J_{i_1 \cdots i_q}^{(L)} = J_{i_1 \cdots i_q}^{(R)}$ are written in the basis (B.3) as

$$H_{\text{SYK}}^{(L)} = H_{\text{SYK}} \otimes 1, \quad H_{\text{SYK}}^{(R)} = 1 \otimes H_{\text{SYK}}, \tag{B.8}$$

with

$$H_{\text{SYK}} = \frac{1}{2^{\frac{q}{2}}} i^{\frac{q}{2}} \sum_{i_1 < \cdots < i_q} J_{i_1 \cdots i_q}^{(L)} \gamma_{i_1} \cdots \gamma_{i_q}. \tag{B.9}$$

Since H_{SYK} commutes with γ_c, we can choose the eigenstates of H_{SYK} as simultaneous eigenstates of γ_c. Also, since H_{SYK} commutes with C, we can classify these eigenstates by using C. As the relations (B.6) suggest, the classification, as well as the consequent expression of $|I\rangle$, depends on N mod 8.

[7] We have chosen the convention of Γ_c so that the fermion number of the two-coupled system always coincides with the sum of the fermion numbers of each side for any $N \in 2\mathbb{N}$. Note that our choice is different from the one $\Gamma_c^{(\text{another})} = (-4)^{\frac{N}{2}} \psi_1^{(L)} \psi_1^{(R)} \psi_2^{(L)} \psi_2^{(R)} \cdots \psi_N^{(L)} \psi_N^{(R)}$ with which the fermion parity of $|I\rangle$ is independent of N: $\Gamma_c^{(\text{another})}|I\rangle = |I\rangle$.

JHEP04(2023)145

B.2.1 $q = 0$ **mod** 4, $N = 0$ **mod** 8

First let us consider the case $q = 0$ mod 4 and $N = 0$ mod 8. In this case γ_c and C commute with each other. Therefore, if $|n, \sigma\rangle$ is an eigenstate of $H_{\rm SYK}$ with $H_{\rm SYK} = E_{n,\sigma}$ and $\gamma_c = \sigma$, $C|n, \sigma\rangle$ is also an eigenstate of $H_{\rm SYK}, \gamma_c$ with $H_{\rm SYK} = E_{n,\sigma}$ and $\gamma_c = \sigma$. Moreover, since $C^2 = 1$, we can choose the eigenstates $|n, \sigma\rangle$ such that $C|n, \sigma\rangle = |n, \sigma\rangle$: if $C|n, \sigma\rangle \neq |n, \sigma\rangle$ we can redefine $(|n, \sigma\rangle + C|n, \sigma\rangle) \times$(real number) and/or $i(|n, \sigma\rangle - C|n, \sigma\rangle) \times$(real number) as $|n, \sigma\rangle$. It turns out that there are no degeneracies with generic $J^{(L)}_{i_1 \cdots i_q}$, hence the eigenstates of $H_{\rm SYK}$ are summarized as

eigenstates of $H_{\rm SYK}$	γ_c	$H_{\rm SYK}$
$\|n, +\rangle \quad (C\|n, +\rangle = \|n, +\rangle;\ n = 1, 2, \cdots, 2^{N/2-1})$	$+1$	$E_{n,+}$
$\|n, -\rangle \quad (C\|n, +\rangle = \|n, -\rangle;\ n = 1, 2, \cdots, 2^{N/2-1})$	-1	$E_{n,-}$

, (B.10)

where $E_{n,+} \neq E_{n,-}$.

Since $|I\rangle$ satisfies $\Gamma^{(R)}_i |I\rangle = i\Gamma^{(L)}_i |I\rangle$, we have $H^{(L)}_{\rm SYK}|I\rangle = H^{(R)}_{\rm SYK}|I\rangle$, which suggests that $|I\rangle$ is expanded as

$$|I\rangle = \sum_{n=1}^{2^{N/2-1}} \sum_{\sigma=\pm 1} a_{n,\sigma} |n, \sigma\rangle \otimes |n, \sigma\rangle. \tag{B.11}$$

Since the ground state of $H_{\rm int}$ is non-degenerate, $a_{n,\sigma}$ can be determined uniquely by solving $\langle I|H_{\rm int}|I\rangle = -\frac{N}{2}$. By using the explicit expressions of $\Gamma^{(L)}_i, \Gamma^{(R)}_i$ (B.3) and the properties of $|n, \sigma\rangle$ under C, γ_c we can rewrite $\langle I|H_{\rm int}|I\rangle$ as

$$\begin{aligned}
\langle I|H_{\rm int}|I\rangle &= \frac{i}{2} \sum_{i=1}^{N} \sum_{m,n} \sum_{\sigma} a^*_{m,\sigma} a_{n,-\sigma} \langle m, \sigma|\gamma_i \gamma_c|n, -\sigma\rangle \langle m, \sigma|\gamma_i|n, -\sigma\rangle \\
&= \frac{i}{2} \sum_{i=1}^{N} \sum_{m,n} \sum_{\sigma} (-\sigma) a^*_{m,\sigma} a_{n,-\sigma} \langle m, \sigma|\gamma_i|n, -\sigma\rangle \langle m, \sigma|\gamma_i|n, -\sigma\rangle \\
&= \frac{i}{2} \sum_{i=1}^{N} \sum_{m,n} \sum_{\sigma} (-\sigma) a^*_{m,\sigma} a_{n,-\sigma} \langle m, \sigma|\gamma_i|n, -\sigma\rangle \langle n, -\sigma|\gamma_i|m, \sigma\rangle,
\end{aligned} \tag{B.12}$$

where in the first line we have used the fact that γ_i flip the fermion number parity γ_c and in the third line we have used the formula (B.7). If we assume $a_{n,\sigma} = a_\sigma$ is independent of n, we can use the fact that $\{|n, \sigma\rangle\}$ is a complete orthonormal basis, i.e., $\sum_{n,\sigma'} |n, \sigma'\rangle\langle n, \sigma'| = 1$, to further simplify the right-hand side of (B.12):

$$\langle I|H_{\rm int}|I\rangle = \frac{i}{2} \sum_{i=1}^{N} \sum_{m} \sum_{\sigma} (-\sigma) a^*_\sigma a_{-\sigma} \langle m, \sigma|\gamma_i \gamma_i|m, \sigma\rangle = -2^{N/2-2} iN \sum_{\sigma=\pm 1} \sigma a^*_\sigma a_{-\sigma}. \tag{B.13}$$

Hence from $\langle I|H_{\rm int}|I\rangle = -\frac{N}{2}$ we obtain the condition $2^{N/2-1} \sum_\sigma \sigma a^*_\sigma a_{-\sigma} = -i$. Combining this with the normalization condition $\langle I|I\rangle = 2^{N/2-1} \sum_\sigma |a_\sigma|^2 = 1$, we can determine a_σ as $(a_+, a_-) = (2^{-N/4}, -2^{-N/4} i)$ up to an overall phase. After all, we obtain the following expression for $|I\rangle$:

$$|I\rangle_{q=0 \text{ mod } 4, N=0 \text{ mod } 8} = 2^{-\frac{N}{4}} \sum_{n=1}^{2^{\frac{N}{2}-1}} (|n, +\rangle \otimes |n, +\rangle - i|n, -\rangle \otimes |n, -\rangle). \tag{B.14}$$

JHEP04(2023)145

B.2.2 $q = 0$ **mod** 4, $N = 2, 6$ **mod** 8

In this case γ_c anti-commutes with C. Hence if $|n, +\rangle$ is an eigenstate of $H_{\rm SYK}$ with $H_{\rm SYK} = E_n$ and $\gamma_c = +1$, $C|n, +\rangle$ is another eigenstate of $H_{\rm SYK}$ with $H_{\rm SYK} = E_n$ and $\gamma_c = -1$, i.e., the spectrum is degenerate between $\gamma_c = \pm 1$ sectors and summarized as follows

eigenstates of $H_{\rm SYK}$	γ_c	$H_{\rm SYK}$
$\|n, +\rangle \quad (n = 1, 2, \cdots, 2^{N/2-1})$	$+1$	E_n
$C\|n, +\rangle \quad (n = 1, 2, \cdots, 2^{N/2-1})$	-1	E_n

. (B.15)

Taking into account the fact that $H^{(L)}_{\rm SYK}|I\rangle = H^{(R)}_{\rm SYK}|I\rangle$ together with $\Gamma_c|I\rangle = -|I\rangle$, we pose the following ansatz:

$$|I\rangle = \sum_{n=1}^{2^{N/2-1}} (a_{n,+}|n, +\rangle \otimes C|n, +\rangle + a_{n,-}C|n, +\rangle \otimes |n, +\rangle), \tag{B.16}$$

where we have defined $|n, -\rangle = C|n, +\rangle$. By imposing $\langle I|H_{\rm int}|I\rangle = -\frac{N}{2}$ and $\langle I|I\rangle = 1$ we can determine $a_{n,\sigma}$ and obtain the following expressions:

$$\begin{aligned}
|I\rangle_{q=0 \text{ mod } 4, N=2 \text{ mod } 8} &= 2^{-\frac{N}{4}} \sum_{n=1}^{2^{\frac{N}{2}-1}} (|n, +\rangle \otimes C|n, +\rangle - iC|n, +\rangle \otimes |n, +\rangle), \\
|I\rangle_{q=0 \text{ mod } 4, N=6 \text{ mod } 8} &= 2^{-\frac{N}{4}} \sum_{n=1}^{2^{\frac{N}{2}-1}} (|n, +\rangle \otimes C|n, +\rangle + iC|n, +\rangle \otimes |n, +\rangle).
\end{aligned} \tag{B.17}$$

B.2.3 $q = 0$ **mod** 4, $N = 4$ **mod** 8

In this case γ_c commutes with C, hence $|n, \sigma\rangle$ and $C|n, \sigma\rangle$ have the same eigenvalues both for $H_{\rm SYK}$ and γ_c. In contrast to the case $N = 0$ mod 8, since $C^2 = -1$ it is impossible to have a state $|\phi\rangle$ as $C|\phi\rangle = |\phi\rangle$. This implies that there are two-fold degeneracy within each of $\gamma_c = \pm 1$ sector. In summary,

eigenstates of $H_{\rm SYK}$	γ_c	$H_{\rm SYK}$
$\|n, +\rangle \quad (n = 1, 2, \cdots, 2^{N/2-2})$	$+1$	$E_{n,+}$
$C\|n, +\rangle \quad (n = 1, 2, \cdots, 2^{N/2-2})$	$+1$	$E_{n,+}$
$\|n, -\rangle \quad (n = 1, 2, \cdots, 2^{N/2-2})$	-1	$E_{n,-}$
$C\|n, -\rangle \quad (n = 1, 2, \cdots, 2^{N/2-2})$	-1	$E_{n,-}$

. (B.18)

Taking into account $H^{(L)}_{\rm SYK}|I\rangle = H^{(R)}_{\rm SYK}|I\rangle$ and $\Gamma_c|I\rangle = |I\rangle$, we pose the following ansatz for $|I\rangle$:

$$\begin{aligned}
|I\rangle = \sum_{n=1}^{2^{N/2-2}} \sum_{\sigma=\pm} &(a_{n,\sigma}|n, \sigma\rangle \otimes |n, \sigma\rangle + b_{n,\sigma}|n, \sigma\rangle \otimes C|n, \sigma\rangle \\
&+ c_{n,\sigma}C|n, \sigma\rangle \otimes |n, \sigma\rangle + d_{n,\sigma}C|n, \sigma\rangle \otimes C|n, \sigma\rangle).
\end{aligned} \tag{B.19}$$

JHEP04(2023)145

By imposing $\langle I|H_{\rm int}|I\rangle = -\frac{N}{2}$ and $\langle I|I\rangle = 1$ we can determine $a_{n,\sigma}, b_{n,\sigma}, c_{n,\sigma}, d_{n,\sigma}$ and obtain the following expression:

$$|I\rangle_{q=0 \text{ mod } 4, N=4 \text{ mod } 8}$$
$$= 2^{-\frac{N}{4}} \sum_{n=1}^{2^{\frac{N}{2}-2}} \Big(|n,+\rangle \otimes C|n,+\rangle - C|n,+\rangle \otimes |n,+\rangle - i(|n,-\rangle \otimes C|n,-\rangle - C|n,-\rangle \otimes |n,-\rangle) \Big). \tag{B.20}$$

B.3 $q = 2$ mod 4

For $q = 2$ mod 4, $H^{(L)}_{\rm SYK}$ and $H^{(R)}_{\rm SYK}$ with $J^{(L)}_{i_1\cdots i_q} = J^{(R)}_{i_1\cdots i_q}$ are written in the basis (B.3) as

$$H^{(L)}_{\rm SYK} = H_{\rm SYK} \otimes 1, \quad H^{(R)}_{\rm SYK} = -1 \otimes H_{\rm SYK}, \tag{B.21}$$

with

$$H_{\rm SYK} = \frac{1}{2^{\frac{q}{2}}} i^{\frac{q}{2}} \sum_{i_1<\cdots<i_q} J^{(L)}_{i_1\cdots i_q} \gamma_{i_1} \cdots \gamma_{i_q}. \tag{B.22}$$

For $q = 2$ mod 4, $H_{\rm SYK}$ does not commute with C due to the factor $i^{\frac{q}{2}}$. Nevertheless, since $H_{\rm SYK}$ anti-commutes with C, an eigenstate of $H_{\rm SYK}$ with eigenvalue E_n transforms to another eigenstate of $H_{\rm SYK}$ with eigenvalue $-E_n$ and C is still useful to classify the eigenstates of $H_{\rm SYK}$.

B.3.1 $q = 2$ mod 4, $N = 0, 4$ mod 8

Since γ_c and C commute, we obtain the following classification of the spectrum of single $H_{\rm SYK}$:

eigenstates of $H_{\rm SYK}$	γ_c	$H_{\rm SYK}$
$\|n,+\rangle \quad (n = 1, 2, \cdots, 2^{N/2-2})$	$+1$	$E_{n,+}$
$C\|n,+\rangle \quad (n = 1, 2, \cdots, 2^{N/2-2})$	$+1$	$-E_{n,+}$
$\|n,-\rangle \quad (n = 1, 2, \cdots, 2^{N/2-2})$	-1	$E_{n,-}$
$C\|n,-\rangle \quad (n = 1, 2, \cdots, 2^{N/2-2})$	-1	$-E_{n,-}$

. (B.23)

There are no degeneracy for generic $J^{(L)}_{i_1\cdots i_q}$.

To write down an ansatz for $|I\rangle$ notice that $i\Gamma^{(L)}_i \Gamma^{(R)}_i |I\rangle = |I\rangle$ implies $(H_{\rm SYK} \otimes 1)|I\rangle = -(1 \otimes H_{\rm SYK})|I\rangle$ for $q = 2$ mod 4. Hence we need to pair an energy eigenstate of single side with $H_{\rm SYK} = E$ and a different energy eigenstate with $H_{\rm SYK} = -E$. Taking this into account together with the classification (B.23) we pose the following ansatz:

$$|I\rangle = \sum_{n=1}^{2^{\frac{N}{2}-2}} \sum_{\sigma} (a_{n,\sigma}|n,\sigma\rangle \otimes C|n,\sigma\rangle + b_{n,\sigma} C|n,\sigma\rangle \otimes |n,\sigma\rangle). \tag{B.24}$$

JHEP04(2023)145

Now we can determine the coefficients $a_{m,\sigma}, b_{m,\sigma}$ by completely the same strategy as we have used for $q = 4$, and we obtain

$$
\begin{aligned}
&|I\rangle_{q=2 \text{ mod } 4, N=0 \text{ mod } 8} \\
&= 2^{-\frac{N}{4}} \sum_{n=1}^{2^{\frac{N}{2}-2}} \Big(|n,+\rangle\otimes C|n,+\rangle + C|n,+\rangle\otimes|n,+\rangle - i(|n,-\rangle\otimes C|n,-\rangle + C|n,-\rangle\otimes|n,-\rangle) \Big), \\
&|I\rangle_{q=2 \text{ mod } 4, N=4 \text{ mod } 8} \\
&= 2^{-\frac{N}{4}} \sum_{n=1}^{2^{\frac{N}{2}-2}} \Big(|n,+\rangle\otimes C|n,+\rangle - C|n,+\rangle\otimes|n,+\rangle - i(|n,-\rangle\otimes C|n,-\rangle - C|n,-\rangle\otimes|n,-\rangle) \Big).
\end{aligned}
\tag{B.25}
$$

B.3.2 $q = 2$ mod 4, $N = 2, 6$ mod 8

Since γ_c and C anti-commute, we obtain the following classification of the spectrum of single H_{SYK}:

eigenstates of H_{SYK}	γ_c	H_{SYK}
$\|n,+\rangle \quad (n = 1, 2, \cdots, 2^{N/2-1})$	$+1$	E_n
$C\|n,+\rangle \quad (n = 1, 2, \cdots, 2^{N/2-1})$	-1	$-E_n$

(B.26)

There are no degeneracy for generic $J^{(L)}_{i_1\cdots i_q}$.

By posing the following ansatz

$$
|I\rangle = \sum_{n=1}^{2^{\frac{N}{2}-1}} (a_{n,+}|n,+\rangle\otimes C|n,+\rangle + a_{n,-}C|n,+\rangle\otimes|n,+\rangle),
\tag{B.27}
$$

we obtain $|I\rangle$ as

$$
\begin{aligned}
|I\rangle_{q=2 \text{ mod } 4, N=2 \text{ mod } 8} &= 2^{-\frac{N}{4}} \sum_{n=1}^{2^{\frac{N}{2}-1}} (|n,+\rangle\otimes C|n,+\rangle - iC|n,+\rangle\otimes|n,+\rangle), \\
|I\rangle_{q=2 \text{ mod } 4, N=6 \text{ mod } 8} &= 2^{-\frac{N}{4}} \sum_{n=1}^{2^{\frac{N}{2}-1}} (|n,+\rangle\otimes C|n,+\rangle + iC|n,+\rangle\otimes|n,+\rangle).
\end{aligned}
\tag{B.28}
$$

References

[1] S. Sachdev and J. Ye, *Gapless spin fluid ground state in a random, quantum Heisenberg magnet*, *Phys. Rev. Lett.* **70** (1993) 3339 [cond-mat/9212030] [INSPIRE].

[2] A. Kitaev, *A simple model of quantum holography*, talk at *KITP strings seminar and Entanglement 2015 program* (2015), http://online.kitp.ucsb.edu/online/entangled15/.

JHEP04(2023)145

[3] J. Maldacena, D. Stanford and Z. Yang, *Conformal symmetry and its breaking in two dimensional Nearly Anti-de-Sitter space*, *PTEP* **2016** (2016) 12C104 [arXiv:1606.01857] [INSPIRE].

[4] W. Israel, *Thermo field dynamics of black holes*, *Phys. Lett. A* **57** (1976) 107 [INSPIRE].

[5] J.M. Maldacena, *Eternal black holes in anti-de Sitter*, *JHEP* **04** (2003) 021 [hep-th/0106112] [INSPIRE].

[6] M. Van Raamsdonk, *Building up spacetime with quantum entanglement*, *Gen. Rel. Grav.* **42** (2010) 2323 [arXiv:1005.3035] [INSPIRE].

[7] S. Ryu and T. Takayanagi, *Holographic derivation of entanglement entropy from AdS/CFT*, *Phys. Rev. Lett.* **96** (2006) 181602 [hep-th/0603001] [INSPIRE].

[8] V.E. Hubeny, M. Rangamani and T. Takayanagi, *A Covariant holographic entanglement entropy proposal*, *JHEP* **07** (2007) 062 [arXiv:0705.0016] [INSPIRE].

[9] N. Engelhardt and A.C. Wall, *Quantum Extremal Surfaces: Holographic Entanglement Entropy beyond the Classical Regime*, *JHEP* **01** (2015) 073 [arXiv:1408.3203] [INSPIRE].

[10] J. Maldacena and L. Susskind, *Cool horizons for entangled black holes*, *Fortsch. Phys.* **61** (2013) 781 [arXiv:1306.0533] [INSPIRE].

[11] B. Swingle, *Constructing holographic spacetimes using entanglement renormalization*, arXiv:1209.3304 [INSPIRE].

[12] S.R. Coleman, *Black Holes as Red Herrings: Topological Fluctuations and the Loss of Quantum Coherence*, *Nucl. Phys. B* **307** (1988) 867 [INSPIRE].

[13] S.B. Giddings and A. Strominger, *Loss of Incoherence and Determination of Coupling Constants in Quantum Gravity*, *Nucl. Phys. B* **307** (1988) 854 [INSPIRE].

[14] S.B. Giddings and A. Strominger, *Axion Induced Topology Change in Quantum Gravity and String Theory*, *Nucl. Phys. B* **306** (1988) 890 [INSPIRE].

[15] P. Saad, S.H. Shenker, D. Stanford and S. Yao, *Wormholes without averaging*, arXiv:2103.16754 [INSPIRE].

[16] P. Saad, S. Shenker and S. Yao, *Comments on wormholes and factorization*, arXiv:2107.13130 [INSPIRE].

[17] A. Almheiri, T. Hartman, J. Maldacena, E. Shaghoulian and A. Tajdini, *Replica Wormholes and the Entropy of Hawking Radiation*, *JHEP* **05** (2020) 013 [arXiv:1911.12333] [INSPIRE].

[18] G. Penington, S.H. Shenker, D. Stanford and Z. Yang, *Replica wormholes and the black hole interior*, *JHEP* **03** (2022) 205 [arXiv:1911.11977] [INSPIRE].

[19] A. Kundu, *Wormholes and holography: an introduction*, *Eur. Phys. J. C* **82** (2022) 447 [arXiv:2110.14958] [INSPIRE].

[20] P. Betzios, E. Kiritsis and O. Papadoulaki, *Euclidean Wormholes and Holography*, *JHEP* **06** (2019) 042 [arXiv:1903.05658] [INSPIRE].

[21] P. Betzios, E. Kiritsis and O. Papadoulaki, *Interacting systems and wormholes*, *JHEP* **02** (2022) 126 [arXiv:2110.14655] [INSPIRE].

[22] M. Van Raamsdonk, *Comments on wormholes, ensembles, and cosmology*, *JHEP* **12** (2021) 156 [arXiv:2008.02259] [INSPIRE].

JHEP04(2023)145

[23] Y. Chen, V. Gorbenko and J. Maldacena, *Bra-ket wormholes in gravitationally prepared states*, *JHEP* **02** (2021) 009 [arXiv:2007.16091] [INSPIRE].

[24] T. Numasawa, *Four coupled SYK models and nearly AdS_2 gravities: phase transitions in traversable wormholes and in bra-ket wormholes*, *Class. Quant. Grav.* **39** (2022) 084001 [arXiv:2011.12962] [INSPIRE].

[25] J.M. Maldacena and L. Maoz, *Wormholes in AdS*, *JHEP* **02** (2004) 053 [hep-th/0401024] [INSPIRE].

[26] D. Bak, M. Gutperle and S. Hirano, *Three dimensional Janus and time-dependent black holes*, *JHEP* **02** (2007) 068 [hep-th/0701108] [INSPIRE].

[27] D. Bak, M. Gutperle and R.A. Janik, *Janus Black Holes*, *JHEP* **10** (2011) 056 [arXiv:1109.2736] [INSPIRE].

[28] Y. Nakaguchi, N. Ogawa and T. Ugajin, *Holographic Entanglement and Causal Shadow in Time-Dependent Janus Black Hole*, *JHEP* **07** (2015) 080 [arXiv:1412.8600] [INSPIRE].

[29] A. Goel, H.T. Lam, G.J. Turiaci and H. Verlinde, *Expanding the Black Hole Interior: Partially Entangled Thermal States in SYK*, *JHEP* **02** (2019) 156 [arXiv:1807.03916] [INSPIRE].

[30] D. Bak, M. Gutperle and A. Karch, *Time dependent black holes and thermal equilibration*, *JHEP* **12** (2007) 034 [arXiv:0708.3691] [INSPIRE].

[31] J. Maldacena and X.-L. Qi, *Eternal traversable wormhole*, arXiv:1804.00491 [INSPIRE].

[32] P. Gao, D.L. Jafferis and A.C. Wall, *Traversable Wormholes via a Double Trace Deformation*, *JHEP* **12** (2017) 151 [arXiv:1608.05687] [INSPIRE].

[33] P. Gao and H. Liu, *Regenesis and quantum traversable wormholes*, *JHEP* **10** (2019) 048 [arXiv:1810.01444] [INSPIRE].

[34] A.M. García-García, T. Nosaka, D. Rosa and J.J.M. Verbaarschot, *Quantum chaos transition in a two-site Sachdev-Ye-Kitaev model dual to an eternal traversable wormhole*, *Phys. Rev. D* **100** (2019) 026002 [arXiv:1901.06031] [INSPIRE].

[35] F. Alet, M. Hanada, A. Jevicki and C. Peng, *Entanglement and Confinement in Coupled Quantum Systems*, *JHEP* **02** (2021) 034 [arXiv:2001.03158] [INSPIRE].

[36] T. Nosaka and T. Numasawa, *Quantum Chaos, Thermodynamics and Black Hole Microstates in the mass deformed SYK model*, *JHEP* **08** (2020) 081 [arXiv:1912.12302] [INSPIRE].

[37] T. Nosaka and T. Numasawa, *Chaos exponents of SYK traversable wormholes*, *JHEP* **02** (2021) 150 [arXiv:2009.10759] [INSPIRE].

[38] A.M. García-García, Y. Jia, D. Rosa and J.J.M. Verbaarschot, *Dominance of Replica Off-Diagonal Configurations and Phase Transitions in a PT Symmetric Sachdev-Ye-Kitaev Model*, *Phys. Rev. Lett.* **128** (2022) 081601 [arXiv:2102.06630] [INSPIRE].

[39] A.M. García-García, Y. Jia, D. Rosa and J.J.M. Verbaarschot, *Replica symmetry breaking in random non-Hermitian systems*, *Phys. Rev. D* **105** (2022) 126027 [arXiv:2203.13080] [INSPIRE].

[40] A.M. García-García, V. Godet, C. Yin and J.P. Zheng, *Euclidean-to-Lorentzian wormhole transition and gravitational symmetry breaking in the Sachdev-Ye-Kitaev model*, *Phys. Rev. D* **106** (2022) 046008 [arXiv:2204.08558] [INSPIRE].

[41] N. Sorokhaibam, *Traversable wormhole without interaction*, arXiv:2007.07169 [INSPIRE].

JHEP04(2023)145

[42] W. Cai, S. Cao, X.-H. Ge, M. Matsumoto and S.-J. Sin, *Non-Hermitian quantum system generated from two coupled Sachdev-Ye-Kitaev models*, *Phys. Rev. D* **106** (2022) 106010 [arXiv:2208.10800] [INSPIRE].

[43] S. Sachdev, *Bekenstein-Hawking Entropy and Strange Metals*, *Phys. Rev. X* **5** (2015) 041025 [arXiv:1506.05111] [INSPIRE].

[44] A.M. García-García, J.P. Zheng and V. Ziogas, *Phase diagram of a two-site coupled complex SYK model*, *Phys. Rev. D* **103** (2021) 106023 [arXiv:2008.00039] [INSPIRE].

[45] H. Rathi and D. Roychowdhury, *Phases of complex SYK from Euclidean wormholes*, arXiv:2111.11279 [INSPIRE].

[46] I. Kourkoulou and J. Maldacena, *Pure states in the SYK model and nearly-AdS_2 gravity*, arXiv:1707.02325 [INSPIRE].

[47] S. Plugge, E. Lantagne-Hurtubise and M. Franz, *Revival Dynamics in a Traversable Wormhole*, *Phys. Rev. Lett.* **124** (2020) 221601 [arXiv:2003.03914] [INSPIRE].

[48] A.I. Larkin and Y.N. Ovchinnikov, *Quasiclassical Method in the Theory of Superconductivity*, *Sov. J. Exp. Theor. Phys.* **28** (1969) 1200.

[49] X.-L. Qi and P. Zhang, *The Coupled SYK model at Finite Temperature*, *JHEP* **05** (2020) 129 [arXiv:2003.03916] [INSPIRE].

[50] A. Almheiri and H.W. Lin, *The entanglement wedge of unknown couplings*, *JHEP* **08** (2022) 062 [arXiv:2111.06298] [INSPIRE].

[51] A. Streicher, *SYK Correlators for All Energies*, *JHEP* **02** (2020) 048 [arXiv:1911.10171] [INSPIRE].

[52] T. Kanazawa and T. Wettig, *Complete random matrix classification of SYK models with $\mathcal{N} = 0$, 1 and 2 supersymmetry*, *JHEP* **09** (2017) 050 [arXiv:1706.03044] [INSPIRE].

[53] R. Haenel, S. Sahoo, T.H. Hsieh and M. Franz, *Traversable wormhole in coupled Sachdev-Ye-Kitaev models with imbalanced interactions*, *Phys. Rev. B* **104** (2021) 035141 [arXiv:2102.05687] [INSPIRE].

[54] A.M. García-García, Y. Jia, D. Rosa and J.J.M. Verbaarschot, *Sparse Sachdev-Ye-Kitaev model, quantum chaos and gravity duals*, *Phys. Rev. D* **103** (2021) 106002 [arXiv:2007.13837] [INSPIRE].

[55] S. Xu, L. Susskind, Y. Su and B. Swingle, *A Sparse Model of Quantum Holography*, arXiv:2008.02303 [INSPIRE].

[56] E. Caceres, A. Misobuchi and R. Pimentel, *Sparse SYK and traversable wormholes*, *JHEP* **11** (2021) 015 [arXiv:2108.08808] [INSPIRE].

[57] A.B. Zamolodchikov, *Expectation value of composite field T anti-T in two-dimensional quantum field theory*, hep-th/0401146 [INSPIRE].

[58] F.A. Smirnov and A.B. Zamolodchikov, *On space of integrable quantum field theories*, *Nucl. Phys. B* **915** (2017) 363 [arXiv:1608.05499] [INSPIRE].

[59] A. Cavaglià, S. Negro, I.M. Szécsényi and R. Tateo, *$T\bar{T}$-deformed 2D Quantum Field Theories*, *JHEP* **10** (2016) 112 [arXiv:1608.05534] [INSPIRE].

[60] B. Le Floch and M. Mezei, *KdV charges in $T\bar{T}$ theories and new models with super-Hagedorn behavior*, *SciPost Phys.* **7** (2019) 043 [arXiv:1907.02516] [INSPIRE].

JHEP04(2023)145

[61] S. He and H. Shu, *Correlation functions, entanglement and chaos in the $T\overline{T}/J\overline{T}$-deformed CFTs*, *JHEP* **02** (2020) 088 [arXiv:1907.12603] [INSPIRE].

[62] D.J. Gross, J. Kruthoff, A. Rolph and E. Shaghoulian, *Hamiltonian deformations in quantum mechanics, $T\bar{T}$, and the SYK model*, *Phys. Rev. D* **102** (2020) 046019 [arXiv:1912.06132] [INSPIRE].

[63] G. Jorjadze and S. Theisen, *Canonical maps and integrability in $T\bar{T}$ deformed 2d CFTs*, arXiv:2001.03563 [INSPIRE].

[64] S. He and Z.-Y. Xian, *$T\bar{T}$ deformation on multiquantum mechanics and regenesis*, *Phys. Rev. D* **106** (2022) 046002 [arXiv:2104.03852] [INSPIRE].

JHEP04(2023)145